Coupling of Thermal Mass with Night Ventilation in Buildings

by

Akhilesh Reddy Endurthy

A Thesis Presented in Partial Fulfillment
of the Requirements for the Degree
Master of Science

Approved April 2011 by the
Graduate Supervisory Committee:

T. Agami Reddy, Chair
Marlin Addison
Patrick Phelan

ARIZONA STATE UNIVERSITY

May 2011

ABSTRACT

Passive cooling designs & technologies offer great promise to lower energy use in buildings. Though the working principles of these designs and technologies are well understood, simplified tools to quantitatively evaluate their performance are lacking. Cooling by night ventilation, which is the topic of this research, is one of the well known passive cooling technologies. The building's thermal mass can be cooled at night by ventilating the inside of the space with the relatively lower outdoor air temperatures, thereby maintaining lower indoor temperatures during the warmer daytime period. Numerous studies, both experimental and theoretical, have been performed and have shown the effectiveness of the method to significantly reduce air conditioning loads or improve comfort levels in those climates where the night time ambient air temperature drops below that of the indoor air. The impact of widespread adoption of night ventilation cooling can be substantial, given the large fraction of energy consumed by air conditioning of buildings (about 12-13% of the total electricity use in U.S. buildings). Night ventilation is relatively easy to implement with minimal design changes to existing buildings. Contemporary mathematical models to evaluate the performance of night ventilation are embedded in detailed whole building simulation tools which require a certain amount of expertise and is a time consuming approach.

This research proposes a methodology incorporating two models, Heat Transfer model and Thermal Network model, to evaluate the effectiveness of night ventilation. This methodology is easier to use and the run time to evaluate the results is faster. Both these models are approximations of thermal coupling between thermal mass and night ventilation in buildings. These models are modifications of existing approaches meant to model dynamic thermal response in buildings subject to natural ventilation. Effectiveness of night ventilation was quantified by a parameter called the Discomfort Reduction Factor (DRF) which is the index of reduction of occupant discomfort levels during the day time from night ventilation. Daily and Monthly DRFs are calculated for two climate zones and three building heat capacities. It is verified that night ventilation is effective in seasons and regions when day temperatures are between 30 ^{o}C and 36 ^{o}C and night temperatures are below 20 ^{o}C. The accuracy of these models may be lower than using a detailed simulation program but the loss in accuracy in using these tools more than compensates for the insights provided and better transparency in the analysis approach and results obtained.

ACKNOWLEDGMENTS

I would like to acknowledge my advisor, Dr. Agami Reddy, for his constant encouragement and guidance throughout this research. In addition, I would also like to thank Professor Marlin Addison and Dr. Patrick Phelan for their helpful suggestions during the course of my research. Also, I thank Professor Daniel Feuermann for preliminary discussions related to this topic.

TABLE OF CONTENTS

CHAPTER Page

LIST OF TABLES

LIST OF FIGURES

Figure Page

Figure Page

Figure Page

Figure Page

NOMENCLATURE

A - area of the inner surface of external wall (m^2)

A_i - amplitude of fluctuation of indoor air temperature (^oC)

A_o - amplitude of fluctuation of outdoor air temperature (^oC)

$A_{sol\text{ - }air}$ - amplitude of fluctuation of sol-air temperature (^oC)

C- heat capacity of material (J/kg ^oC)

C_a - heat capacity of air (J/kg ^oC)

C_m - heat capacity of the internal thermal mass (J/kg ^oC)

E - effective total heat power (W)

f_i - decrement factor of indoor air temperature

K - thermal conductivity of material (W/m K)

M - mass of internal thermal mass (kg)

q - ventilation flow rate (m^3/s)

R_o - heat resistance of external wall (m^2 K/W)

t - time (h)

T_E - air temperature rise due to the inner steady state heat source (^oC)

T_i - indoor air temperature (^oC)

T_o, T_a - outdoor air temperature (^oC)

$T_{sol\text{-}air}$ - sol-air temperature (^oC)

T_W - temperature of inner surface of external wall (^oC)

$\bar{T}i$ - mean indoor air temperature (^oC)

$\bar{T}o$ - mean outdoor air temperature (^oC)

$\bar{T}_{sol\_air}$ - mean sol-air temperature (^oC)

$\bar{T}_W$- mean inner surface temperature of external wall (^oC)

α_i - total heat transfer coefficient of inner surface (W/m^2 K)

α_o - total heat transfer coefficient of external surface (W/m^2 K)

λ - heat transfer number

ρ_a - density of air (kg/m^3)

τ/ TC - time constant (h)

υ_e - damping factor of inner surface temperature with respect to sol-air temperature

υ_f - damping factor of inner surface temperature with respect to indoor air temperature

υ_i - damping factor of indoor air temperature with respect to outdoor air temperature

ξ_e - time lag of inner surface temperature with respect to sol-air temperature (h)

ξ_f - time lag of inner surface temperature with respect to indoor air temperature (h)

ξ_i - time lag of indoor air temperature with respect to outdoor air temperature (h)

φ_e - phase shift of inner surface temperature with respect to sol-air temperature (radians)

$\boldsymbol{\varphi}_f$ - phase shift of inner surface temperature with respect to indoor air temperature (radians)

$\boldsymbol{\varphi}_i$ - phase shift of indoor air temperature with respect to outdoor air temperature (radians)

$\boldsymbol{\varphi}_{sol\text{-}air}$ - phase shift of sol-air temperature with respect to outdoor air temperature (radians)

$\boldsymbol{\omega}$ - frequency of outdoor temperature variation (h^{-1})

1. INTRODUCTION

1.1. Overview of passive, hybrid cooling designs and technologies

Passive cooling designs & technologies are those strategies used to cool buildings using natural forces (wind and temperature), with little or no electrical power or gas consumption. Systems with passive cooling strategies partially supplemented by mechanical systems are referred to as hybrid cooling technologies. The implementation of passive and hybrid ventilation presents an opportunity to reduce energy consumption needed for occupant comfort by utilizing free natural cooling as much as possible.

Passive cooling design strategies have long been used historically in buildings especially strategies such as natural ventilation, heavy thermal mass, etc. They were predominant before the advent of mechanical cooling systems. An example of existing ancient architecture where passive cooling designs have been implemented is the Hawa Mahal, also known as "Palace of Winds" or “Palace of the Breeze”, which was built in 18th century in Rajasthan, India and used venturi effect to cool the buildings passively (Figure 1.1). Most of the ancient buildings in tropical climates, such as the Middle East and South Asian countries, were built with higher thermal mass and natural ventilation to maintain cooler interiors (Figure 1.2).

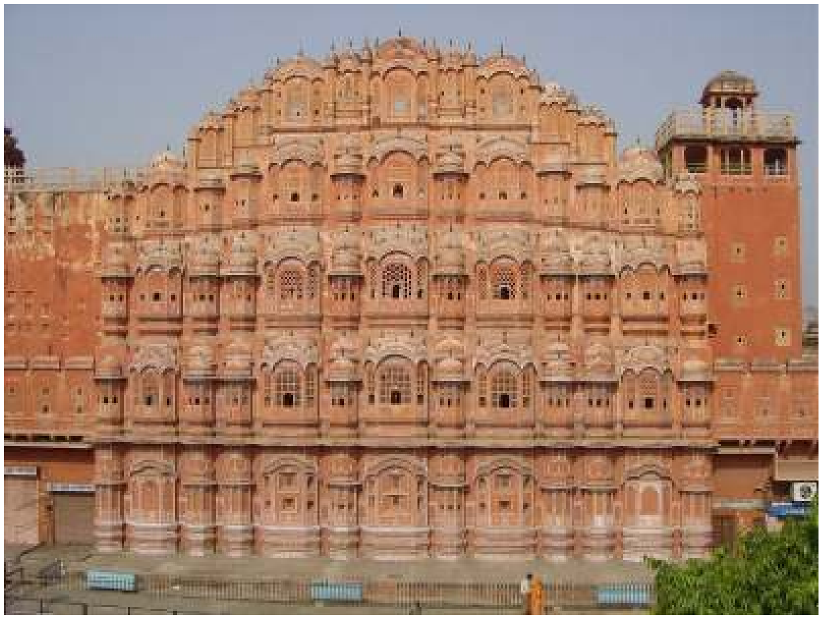

Figure 1.1 – Hawa Mahal (Palace of the Breeze), Rajasthan India where venturi cooling (a passive cooling design) is used. Image courtesy Rajasthan Tourism (http://www.rajasthantourism.gov.in/)

Figure 1.2 – Ancient Persian Architecture with tall wind catchers to cool the interior spaces of the, Borujerdi ha House, in central Iran. Image courtesy Wikipedia.

Commercial and residential buildings consume approximately 72% of the electricity and 39% of primary energy in United States (Buildings Energy Data Book, 2005). Fossil fuel based energy production has adverse consequences in terms of air and water pollution, and climate change; hydro-electric generation plants can make waterways uninhabitable for indigenous fish; and nuclear power has safety concerns as well as problems with disposal of spent fuel.

Of the total energy consumed in buildings, a major portion, around 35% is spent for air-conditioning (both heating and cooling) especially in commercial buildings (Buildings Energy Data Book, 2005). This requires one to look for energy efficient technologies in cooling systems. Use of passive, hybrid cooling designs and technologies can provide a certain amount of occupant comfort while greatly reducing energy use.

1.2. Types of passive, hybrid cooling designs and technologies

Some of the prominent passive, hybrid cooling designs and technologies are described below along with their working principle and operative ambient conditions.

(a) Comfort Ventilation/ Ventilation cooling – This strategy, the simplest of all, is used to improve comfort when indoor temperatures under still conditions, are too warm for occupant comfort. It would be appropriate to define the term ventilation as the supply of outside air to the interior space so as to result in air motion and replacement of still air. Comfort is improved by increasing indoor air velocity. Considering indoor air velocity of 1.5-2 m/s, comfort ventilation is applicable in regions and seasons when the outdoor maximum temperature does not exceed 28 ^{o}C - 32 ^{o}C and the diurnal temperature range is less than 10 ^{o}C, (Givoni, 1994). This can reduce the maximum indoor temperature by about 5 ^{o}C - 8 ^{o}C compared to outdoor air (Nayak and Prajapati, 2006).

Improved indoor thermal comfort through ventilation can be achieved in many ways. For example, to let the wind in, windows can be opened, thus providing a higher indoor air speed; this makes people inside the building feel cooler. This approach is generally termed as "comfort ventilation". In hot environments, the most important process of heat loss from the human body for achieving thermal comfort is evaporation. As the air around the body becomes nearly saturated due to humidity, evaporative cooling from perspiration becomes more difficult and a sense of discomfort is felt. A combination of high humidity and high temperature proves very oppressive. In such circumstances, even a slight movement of air near the body provides relief. Therefore, considering a certain amount of ventilation which may produce necessary air movement is desirable.

If natural ventilation is insufficient, the air movement may be augmented by rotating fans inside the building.

(b) Nocturnal/ Night Ventilative cooling – When a building is night ventilated, its structural mass is cooled by convection from inside, bypassing the thermal resistance of the envelope. During the daytime, this cooled mass, when it has sufficient amount of surface area and if it is adequately insulated from outdoors, can serve as a heat sink through radiation and natural convection.

Thermal mass, which is a function of building construction parameters, may increase the efficiency of night ventilation, since the inertia of the building increases with the increase of thermal mass. The effect of night ventilation can be observed in the next day's indoor temperature profiles, with a lower and delayed peak indoor air temperature. Coupling of thermal mass with night ventilation is analyzed in this study. Previous researchers have stated that night ventilation is applicable to regions where daytime temperatures are between 30 ^{o}C and 36 ^{o}C and the night temperatures are below 20 ^{o}C (Givoni, 1994).

Several design and construction options are available that can provide the thermal mass necessary for nocturnal/ night cool storage. These include mass of the building such as walls, partitions, floors, furniture, etc., embedded air spaces / passages within floors, ceilings and/ or walls through which outdoor air is circulated, specialized storage such as a rock bed or a water tank with embedded air tubes.

Methodology to evaluate night ventilation effectiveness is investigated in the current research. Figure 1.3 is a schematic of night ventilation in buildings showing pathways by which air can be brought indoors and then exhausted through a central location as it gradually heats up. Figure 1.4 is a plot indicating the reduction in amplitude and phase shift in indoor temperature for low and high thermal mass structures.

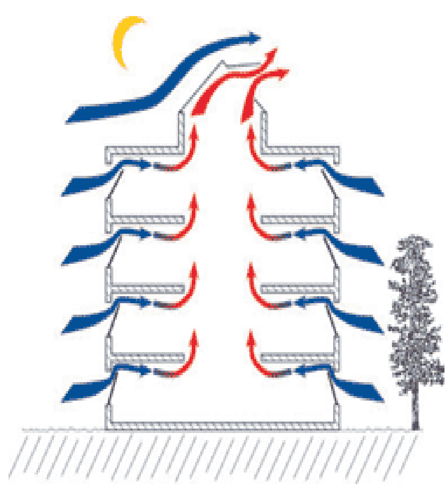

Figure 1.3 – Schematic of night ventilation in buildings. Image courtesy Dyer Environmental Controls

(http://www.dyerenvironmental.co.uk/natural_vent_systems.html)

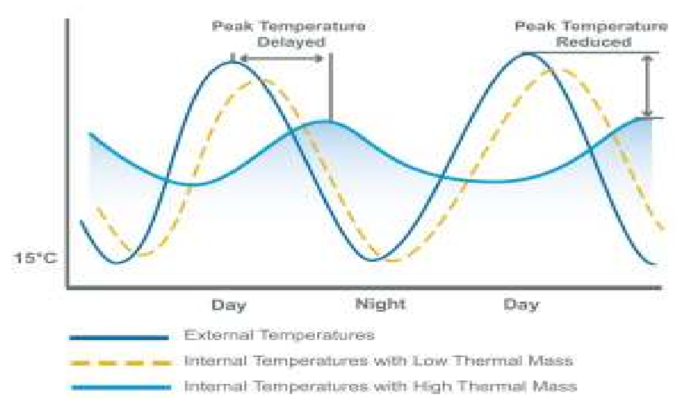

Figure 1.4 – Temperature versus time of data, plotting outdoor temperature, indoor temperature with low and high thermal mass. Image courtesy of MIT OpenCourseWare.

(c) Radiant Cooling – This technology works with the principle of radiant heat loss towards the sky and can be regarded as a heat radiator. The roof which has most exposure to the sky is the natural location for radiant cooling. High-mass roofs with operable insulation provide feasibility for cold collection. Such radiant cooling is effective in providing daytime cooling in almost any region with clear nights.

There are two types of radiant cooling technologies. Brief descriptions of these technologies are as follows.

Massive roofs with movable insulation – Heavy and highly conductive roof exposed to the sky during the night but heavily insulated externally by means of operable insulation during the day time.

The “Skytherm” system – Givoni (1994) states that, in this system roof is made of structural steel deck plates. Above the metal deck, plastic bags filled with water are placed, which are covered with insulation panels that can be moved by a motor to either cover or to expose the bags. In winter, the water bags are exposed to the sun during the day and covered by the insulation panels during the nights. In summer, when cooling is needed, the water bags are exposed and cooled during the night and insulated during the daytime. The cooled water bags are in direct thermal contact with the metal deck, and thus the ceiling serves as a cooling element over the entire space below.

(d) Direct Evaporative Cooling – Mechanical or passively induced air flow through evaporative cooling towers/ devices humidifies the ambient air and thus cools it. Its physical principle lies in the fact that some of the sensible heat of air goes to evaporate water thereby cooling the supply air, which can in turn cool the living space in the building. The efficiency of the evaporation process depends on the temperature of the air and water, the vapor content of the air and the rate of airflow past the water surface. The most common type of evaporative cooling system is the desert cooler consisting of water, evaporative pads, a fan and a pump. It is hybrid type of direct evaporative cooling. Passive down draft evaporative technologies or cooling showers work on the same principle. Figures 1.5 and 1.6 are images of desert coolers and Passive down draft evaporative coolers respectively.

Figure 1.5 – Desert cooler. Image courtesy Zenith home appliances (www. http://zenithhomeappliances.tradeindia.com)

Figure 1.6 – Passive down draft evaporative coolers. Image courtesy hugpages (http://hubpages.com/hub/evaporative-cooling-system-design)

Desert climates are suitable regions for effective use of this strategy. This can be used in places with Wet Bulb Temperature (WBT) of around 24 ^{o}C and the maximum Dry Bulb Temperature (DBT) around 44 ^{o}C, (Givoni, 1994).

(e) The earth as a cooling source – The temperature of the earth's surface is controlled by the ambient conditions. However, the daily as well as seasonal variations of the temperature reduce rapidly with increasing depth from the earth's surface. At depths beyond 4 to 5m, both daily and seasonal fluctuations die out and the seasonal temperature remains almost stable throughout the year and is equal to annual average ambient temperature of that place (Nayak and Prajapati, 2006). The levels of temperature beyond 4 to 5 m depth can be increased by blackened/ glazed earth's surface or can be decreased by shading, white paint, wetted with water spray or by thick vegetation.

This property of uniform temperature beneath the earth's surface can be used for cooling by burying portions of the building underground (called berming) or by using an earth-air pipe system. The later consists of a pipe distributed between the building interiors and a depth 4 to 5 meters beneath the earth's surface. Ambient air is blown through the pipes at one of the ends, which exchanges heat/ cold with the earth's interior and their conditioned air is supplied to the living spaces. Figure 1.7 is a schematic of the earth-air pipe systems. This technique may be more suitable for hot, dry regions with mild winters.

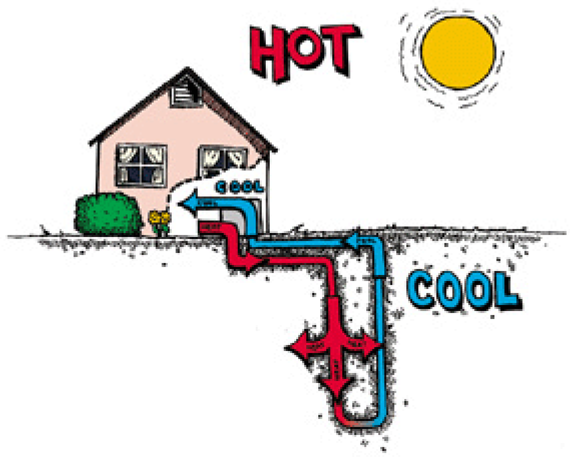

Figure 1.7 – Earth-air pipe system. Image courtesy International Ground Source Heat Pump Association (http://www.igshpa.okstate.edu/geothermal/geothermal.htm)

1.3. Problem statement

Passive cooling designs & technologies have been shown to be proven methods of reducing cooling energy consumption in buildings while maintaining adequate occupant comfort. Though the working principles of these designs and technologies are well understood, simplified tools to quantitatively evaluate the performance of passive cooling technologies are few. This is also the case for night ventilation which is being investigated in this research. Simulation tools are available to evaluate the detailed performance of night ventilation but these may be time consuming to set up and require proper understanding of how to use the software program. Simulation tools which require exhaustive details of the building may be unavailable during the conceptual design stage. Heat transfer models and Thermal network models are simpler and less time consuming approaches which may provide mere insights and a broader understanding of such passive technologies especially at the preliminary stage. The loss of accuracy in using these tools more than compensates for the insights such as analysis periods as well as transparency in the analysis approach. The energy analysts/ architects have to quantify/ weigh the tradeoff between accuracy and cost in time and effort that would be incurred in evaluating passive cooling technologies.

2. OBJECTIVE AND SCOPE

The objective of this research is to identify existing tools, or modify them as appropriate or even develop new ones, in order to evaluate occupant comfort and cooling energy reduction benefits from coupling building thermal mass with night ventilation in residential and commercial buildings. The periods over the year when night ventilation is a valid strategy are to be identified. The heat transfer model developed by Zhou et al. (2008) for natural ventilation in buildings has been modified and used in this research. The thermal network methodology proposed by Feuermann and Hawthorne (1991), in conjunction with various types of thermal networks and their solutions developed by Reddy (1989), have been modified to evaluate performance of coupling of thermal mass and night ventilation in buildings.

eQUEST 3.64 (2010), a whole building energy simulation software program has also been used to evaluate night ventilation performance.

The scope of this research is limited to unconditioned but mechanically ventilated spaces. All the models are evaluated for a sample structure of 50 ft X 50 ft X 10 ft dimensions assumed to be a single zone. A fully mixed space i.e., air temperature uniform throughout zone, is assumed. Effects of only dry bulb temperature are explicitly considered, while humidity effects are ignored. Analysis of the results of the models is done for two similar hot & dry weather locations, Phoenix, AZ and Albuquerque, NM. The effect of thermal mass capacity has been studied by assuming buildings with two time constants representative of the lower and upper values of typical construction. A Discomfort Reduction Factor (DRF) has been proposed so as to quantify the comfort benefits which night ventilation can provide to the occupants. This parameter helps the engineers or architects or building owners to identify the days/ months of the year where night ventilation will be effective. Each of the models used/ developed in this research have certain specific limitations and they are discussed in their respective sections.

3. LITERATURE REVIEW

3.1. Passive, hybrid cooling designs and technologies

The text book by Givoni (1994) and the Handbook on energy conscious buildings by Nayak and Prajapati (2006), describe various passive low energy cooling methods suited for buildings. These books describe various passive and hybrid cooling technologies such as ventilation cooling, evaporative cooling, radiant cooling, desiccant cooling and earth coupling along with their applicability to various climate zones and building types.

As part of understanding, choosing a passive design/ technology and evaluating its performance, the following papers were reviewed. The design and application of natural down-draft evaporative cooling devices has been treated by Chalfoun (1997) who describes the recent developments and applications of cooling towers in arid regions, the use of the CoolT, a computer program developed by the author to design and predict the size of cooling towers. Enhancement of natural ventilation in buildings using a thermal chimney has been studied by Lee and Strand (2008) who developed a model to investigate the effects of chimney height, solar absorptance of the absorber wall, solar transmittance of the glass cover and the air gap width. It is observed that chimney height, solar absorptance and solar transmittance are more influential than the air gap width.

3.2. Indoor thermal comfort conditions

ANSI/ASHRAE Standard 55-2004 deals with occupant comfort in buildings. This standard states that comfort is defined by a range of temperatures rather than a single value. Comfort is defined in terms of “operative temperature”, indoor operative temperature is defined by ANSI/ASHRAE Standard 55-2004, as the uniform temperature of an imaginary black enclosure in which an occupant would exchange the same amount of heat by radiation plus convection as in the actual non-uniform environment. It has been pointed out that for naturally ventilated buildings, indoor operative temperature is dependent on outdoor temperatures as well. Figure 3.1. shows the graph of indoor operative temperatures versus mean monthly outdoor temperatures. In this research indoor operative temperature is simply taken to be the occupant comfort temperature or the set point temperature.

Figure 3.1. is applicable for naturally conditioned spaces, and is of direct relevance to this study since it allows one to determine whether a night ventilation strategy allows the comfort criteria to be met. The relationship between indoor operative temperature – T_i (^oC) and mean monthly outdoor air temperature - T_o (^oC) is given by the equation 3.1.

$$T_i=0.26*T_o+15.5 \qquad (3.1)$$

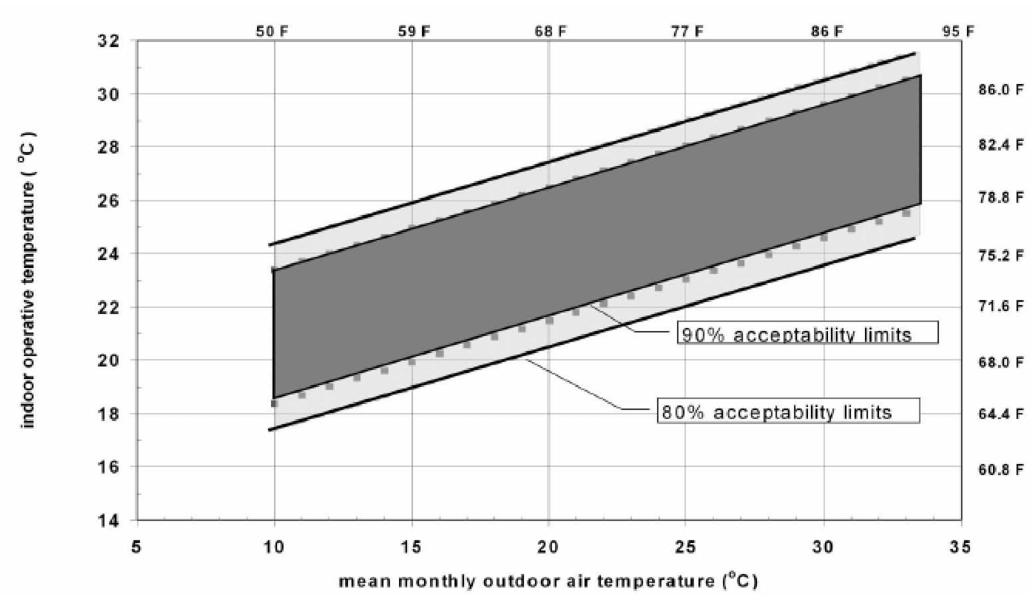

Figure 3.1. – Variation of indoor operative temperature for human comfort with mean monthly outdoor air temperature for naturally ventilated buildings. (ASHRAE Standard 55-2004)

3.3. Night ventilation models

Feuermann and Hawthorne (1991), in their study on the potential and effectiveness of passive night ventilation cooling, proposed a simplified thermal approximation (one capacitor & three resistor networks or 1C3R model) for buildings as shown in Figure 3.2.

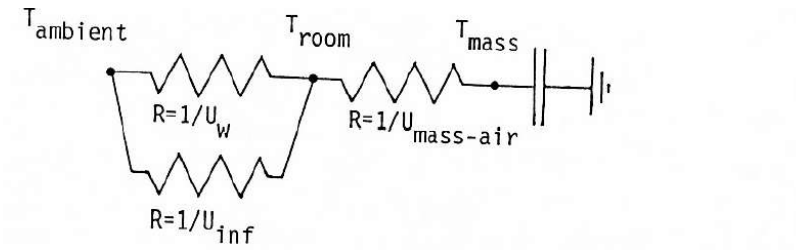

Figure 3.2. Thermal network approximation to study the effect of night ventilation in building (Feuermann and Hawthorne, 1991).

Terms like Potential Cooling Ratio (PCR) and Cooling Efficiency (CE) over a day or over a month are defined as follows where the summations are done at hourly time intervals.

$$CE = \frac{\Sigma(T_{room}-T_{comf})^{+}_{no\ nv} - \Sigma(T_{room}-T_{comf})^{+}_{w\ nv}}{\Sigma(T_{room}-T_{comf})^{+}_{no\ nv}} \qquad (3.2)$$

$$PCR = \frac{(T_{comf} - T_{amb,min})}{(T_{amb,max} - T_{amb,min})} \qquad (3.3)$$

where

T_{room} – Room Temperature

T_{comf} – Occupant comfort temperature

$T_{amb,min}$ – Minimum ambient temperature over day

$T_{amb,max}$ – Maximum ambient temperature over day

no nv – No night ventilation strategy

w nv – Night ventilated strategy

the symbols (+) signify that only positive values add to the summation while (-) negative values are set to zero.

This thermal network did not consider factors like solar radiation, solar aperture and internal heat gain. Further, the network did not give much importance to thermal mass in the exterior building envelope, while assuming internal thermal mass to be dominant. Also, comfort temperature is taken to be a constant value even though the building considered is free floating.

Identification of building parameters using dynamic inverse models was studied by Reddy (1989). Three occupied residences were monitored non-intrusively and corresponding thermal network models and their parameters were inferred. This study did consider the effect of solar radiation and internal heat gains. Figure 3.3, one of several networks studied, was found to be a good representation in many residential buildings. Heat balance equations on the nodes T_i and T_s are given by equation 3.4 and 3.5.

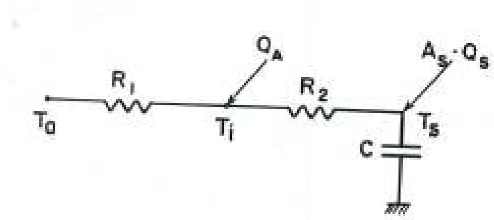

Figure 3.3. A 2R1C electric network to represent building thermal behavior (from Reddy, 1989)

$$\frac{(T_a - T_i)}{R_1} + Q_A = \frac{(T_i - T_s)}{R_2} \tag{3.4}$$

$$C\dot{T}_S = \frac{(T_i - T_s)}{R_2} + A_S . Q_S \tag{3.5}$$

Since T_s is a quantity that is not conveniently measured, this term has to be eliminated. Using equation 3.4 to obtain an expression for T_s which is then substituted for T_s in equation 3.5 and rearranging the terms will yield equation 3.6, which is a first order differential equation with five model parameters $(a_0, b_1, c_0, c_1, d_1)$.

$$\dot{T}_i = a_0 \dot{T}_a + b_1(T_a - T_i) + c_0 \dot{Q}_A + c_1 Q_A + d_1 Q_S \tag{3.6}$$

where

T_i – Indoor air temperature

T_a – Ambient air temperature

T_s- Indoor thermal mass temperature

Q_A - Internal heat gains

Q_S – Solar heat gains

A_S – Area of solar aperture

and the model parameters are given by:

$$a_0 = \frac{R_2}{R_1\left(1 + \frac{R_2}{R_1}\right)}, b_1 = \frac{1}{CR_1\left(1 + \frac{R_2}{R_1}\right)}$$

$$c_0 = \frac{R_2}{\left(1 + \frac{R_2}{R_1}\right)}, c_1 = \frac{1}{C\left(1 + \frac{R_2}{R_1}\right)}, d_1 = \frac{A_S}{C\left(1 + \frac{R_2}{R_1}\right)}$$

The following finite difference scheme has been adapted to discritize equation 3.6.

$$X = \frac{X_{(n)} + X_{(n-1)}}{2} \text{ and } \dot{X} = \frac{X_{(n)} - X_{(n-1)}}{t} \tag{3.7}$$

where t=1 hr.

For naturally ventilated buildings, Zhou et al. (2008) proposed a model to estimate the impact of external and internal thermal mass. Parameters like the time constant of the system, the dimensionless convective heat transfer number and temperature increase induced by internal heat source are used to analyze the effect of thermal mass. This model is an extension of a previous paper by Yam et al. (2003). Using the harmonic response method, the inner surface temperature of external can be estimated. The Zhou et al. (2008) model has been modified so as to predict the indoor air temperature in terms of certain building parameters such as external and internal thermal mass. The model also allows one to determine the amount of internal thermal mass needed to meet a certain pre-stipulated temperature variation range.

Modeling the internal thermal mass by a single capacitor network implies a uniform temperature distribution of the internal thermal mass. Further, the network assumed implies that this thermal mass is equal to indoor air temperature. This makes thermal diffusion heat transfer more dominant than convective heat transfer at the wall surface. This assumption allows calculating the heat exchange between external thermal mass and internal thermal mass, while the radiation between these two bodies can be described by a total heat transfer coefficient. A lumped heat source term, E, is used to represent all sources of heat gain and heat generation in the building. The solar heat gain through apertures and radiation heat exchange between heat source and other surfaces are ignored.

From the above assumption and details, the heat balance at the internal thermal mass can be written as follows (with the corresponding thermal network model shown in Figure 3.4) :

Heat supplied by ventilated air + Heat supplied by external wall + Power from internal heat source generated in the room = Internal energy increases of the internal thermal mass

$$\rho_a C_a q(T_O - T_i) + \alpha_i A(T_w - T_i) + E = MC_m \frac{dT_i}{dt} \tag{3.8}$$

where

$$T_o = \bar{T}_o + A_o \cos[\omega t] \tag{3.9}$$

$$T_{sol-air} = \bar{T}_{sol-air} + A_{sol-air} \cos[\omega t - \varphi_{sol-air}] \tag{3.10}$$

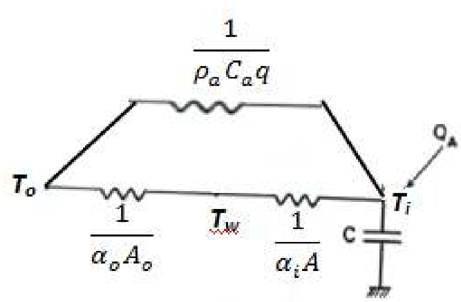

Figure 3.4: Thermal approximation model assumed by Zhou et al. (2008)

Using the harmonic response method, the temperature of the inner surface of external wall T_w is determined as follows:

$$T_w = \overline{T}_w + \frac{A_{sol-air}}{\upsilon_e}\cos[\omega t - \varphi_{sol-air} - \emptyset_e] + \frac{A_i}{\upsilon_f}\cos[\omega t - \varphi_i - \varphi_f] \quad (3.11)$$

The terms on right hand side of the equation denote:

(i) – Average inner surface temperature of external wall,

(ii) – Fluctuation of inner surface caused by the variation of solar-air temperature under constant indoor air condition,

(iii) – Fluctuation of inner surface caused by the variation of indoor air temperature under constant outdoor air temperature condition.

With steady state consideration, the closed form solution of the average inner surface temperature of external wall is

$$\overline{T}_w = \overline{T}_i + \frac{(\overline{T}_{sol-air} - \overline{T}_i)}{\alpha_i R} \quad (3.12)$$

where R is the total thermal resistance and is given by

$$R = \frac{1}{\alpha_o} + R_o + \frac{1}{\alpha_i} \quad (3.13)$$

From the above equations

average indoor air temperature $\overline{T}_i$ is given by

$$\overline{T}_i = \frac{\overline{T}_O + T_E + (\frac{\lambda}{\alpha_i R})\overline{T}_{sol-air}}{1 + (\frac{\lambda}{\alpha_i R})} \quad (3.14)$$

The decrement factor f_i and the time lag ξ_i (in hrs) of indoor air temperature with respect to outdoor air temperature are given by:

$$f_i = \frac{1}{\upsilon_i} = \sqrt{\frac{c^2+d^2}{a^2+b^2}} \tag{3.15}$$

$$\xi_i = \frac{1}{\omega}\tan^{-1}\left(\frac{bc-ad}{ac+bd}\right) \tag{3.16}$$

where

$$a = 1 + \lambda - \frac{\lambda}{\upsilon_f} cos\left(\varphi_f\right)$$
$$b = \frac{\lambda}{\upsilon_f} sin\left(\varphi_f\right) + \tau\omega$$
$$c = -1 - \frac{\lambda}{\upsilon_e} cos(\varphi_{sol-air} + \varphi_e)$$
$$d = \frac{\lambda}{\upsilon_o}\frac{A_{sol-air}}{A_o} sin(\varphi_{sol-air} + \varphi_e)$$

and

$\lambda = \frac{\alpha_i A}{\rho_a C_a q}$ is the convective heat transfer number

$\tau = \frac{MC_m}{\rho_a C_a q}$ is the time constant of the system

$T_E = \frac{E}{\rho_a C_a q}$ is the temperature increase induced by internal heat source.

Finally, all these equations can be combined into an equation for indoor temperature

$$T_i = \overline{T}_i + A_i \cos[\omega(t - \varepsilon_i)] \tag{3.17}$$

3.4. Simulation tools to analyze natural, hybrid ventilation in buildings

A recently completed ASHRAE research project (ASHRAE TRP-1456, 2010) assesses and confines natural and hybrid ventilation models in whole-building energy simulations. The findings are also relevant to our study involving night ventilation which may be considered as a type of hybrid ventilation in buildings. Task 2 of the report reviews and documents existing natural/hybrid ventilation models and simulation tools; While Task 3 discusses model testing and evaluation. The models evaluated in this study are EnergyPlus, COMIS, CONTAM, and ESP-r. The study concludes that all four models are fundamentally similar. It is stated that analytical models developed to date are generally only applicable to specific geometries and specific driving forces. Network airflow models are more appropriate to handle complex interactions between combined driving forces and complex geometries which results in sets of non-linear equations that need to be solved numerically. Analytical models are capable of describing intra-zonal flow characteristics, while network airflow models typically treat each zone as well-mixed. Also, it is stated that a network airflow model may be less accurate for large openings. This report concludes that more experimental data from large openings is needed to prove the relationship.

4. ANALYSIS METHODOLOGY

Methodology used in this research include modifying the heat transfer model developed by Zhou et al. (2008), meant to couple thermal mass and natural ventilation in buildings, so as to apply to night ventilation. Parameters which were constant throughout the day in Zhou et al. (2008) model were varied for hours of the day with and without night ventilation. The indoor temperatures with and without night ventilation are calculated from which daily and monthly values of an index similar to efficiency factor can be deduced.

For the Thermal network model, the methodology proposed by Feuermann and Hawthorne (1991) was used, while the specific thermal network was the one proposed by Reddy (1989). This thermal network model was slightly revised to accommodate night ventilation, and a finite difference scheme was used to numerically solve the differential equation.

A whole building energy simulation model (eQUEST 3.64, 2010) was also used to analyze night ventilation effectiveness.

All these models were used for the test building assumed to be located in two different climates Phoenix, AZ and Albuquerque, NM. The analysis was done for two different values of thermal mass capacitance of the building. Results in terms of daily and monthly Discomfort Reduction Factor (DRF) are compared and analyzed. The reduction in the discomfort (in case there is no A/C) is quantified by a Discomfort Reduction Factor (DRF) as described in equations 4.1 and 4.2. The reduction in A/C electrical use in case such a system is present is quantified by the Cooling Efficiency (CE), defined by equation 3.2.

$$\text{Daily DRF}= \frac{\sum_{24Hrs}(T_{room}-T_{comf})^{+}_{no\ NV}-\sum_{24Hrs}(T_{room}-T_{comf})^{+}_{NV}}{\sum_{24Hrs}(T_{room}-T_{comf})^{+}_{no\ NV}} \tag{4.1}$$

$$\text{Monthly DRF}= \frac{\sum_{30\ days}(T_{room}-T_{comf})^{+}_{no\ NV}-\sum_{30\ days}(T_{room}-T_{comf})^{+}_{NV}}{\sum_{30\ days}(T_{room}-T_{comf})^{+}_{no\ NV}} \tag{4.2}$$

A DRF value of 1 indicates that, with help of night ventilation, 100% indoor comfort can be achieved. A DRF value of 0 indicates that having night ventilation has the same effect on indoor comfort levels and as without night ventilation. To calculate DRF in buildings operating only during certain hours of day, equation 4.1 can be modified by only summing during the period of operating hours rather than 24 hours. In this study, for one of the models, DRF is calculated for the period from 9 AM to 9 PM during which the building is assumed to be occupied, and results are analyzed and compared to DRFs calculated for 24 hours period.

Figure 4.1 is a flow chart of the methodology used in this report. The flow chart describes the inputs to night ventilation models, conditions for the operation of night ventilation and output which is in the form of indoor temperatures with and without implementation of night ventilation strategy and DRF. Night ventilation is only implemented during the hours from 9 PM to 8 AM when buildings have low or no occupants. Further, this period also corresponds to when outdoor temperature is less than comfort temperature and when outdoor temperature is greater than 15 ^{o}C. This limitation on minimum outdoor temperature for operating night ventilation is to prevent overcooling. Overcooling may increase discomfort levels in the spaces.

A MATLAB code was developed for both the Heat Transfer model and the Thermal Network model to calculate indoor air temperature using equations 3.15 and 3.4; Daily and monthly DRF using equations 4.1 and 4.2. MATLAB codes are listed in Appendix A. Table 5.6 lists the inputs and outputs of the MATLAB code.

Table 4.1 – Inputs and outputs of the MATLAB code developed to simulate the Heat Transfer and the Thermal Network models’

Inputs	**Outputs**
Outdoor hourly weather data (Temperature, Windspeed)	Hourly indoor temperatures with and without night ventilation, Cooling Efficiency
Internal heat loads	Daily Discomfort Reduction Factor
Building dimensions	
Day and night Air changes	Monthly Discomfort Reduction Factor (DRF)
Exterior wall's damping factor and time lag	
Interior thermal mass (Volume, density, heat capacity	

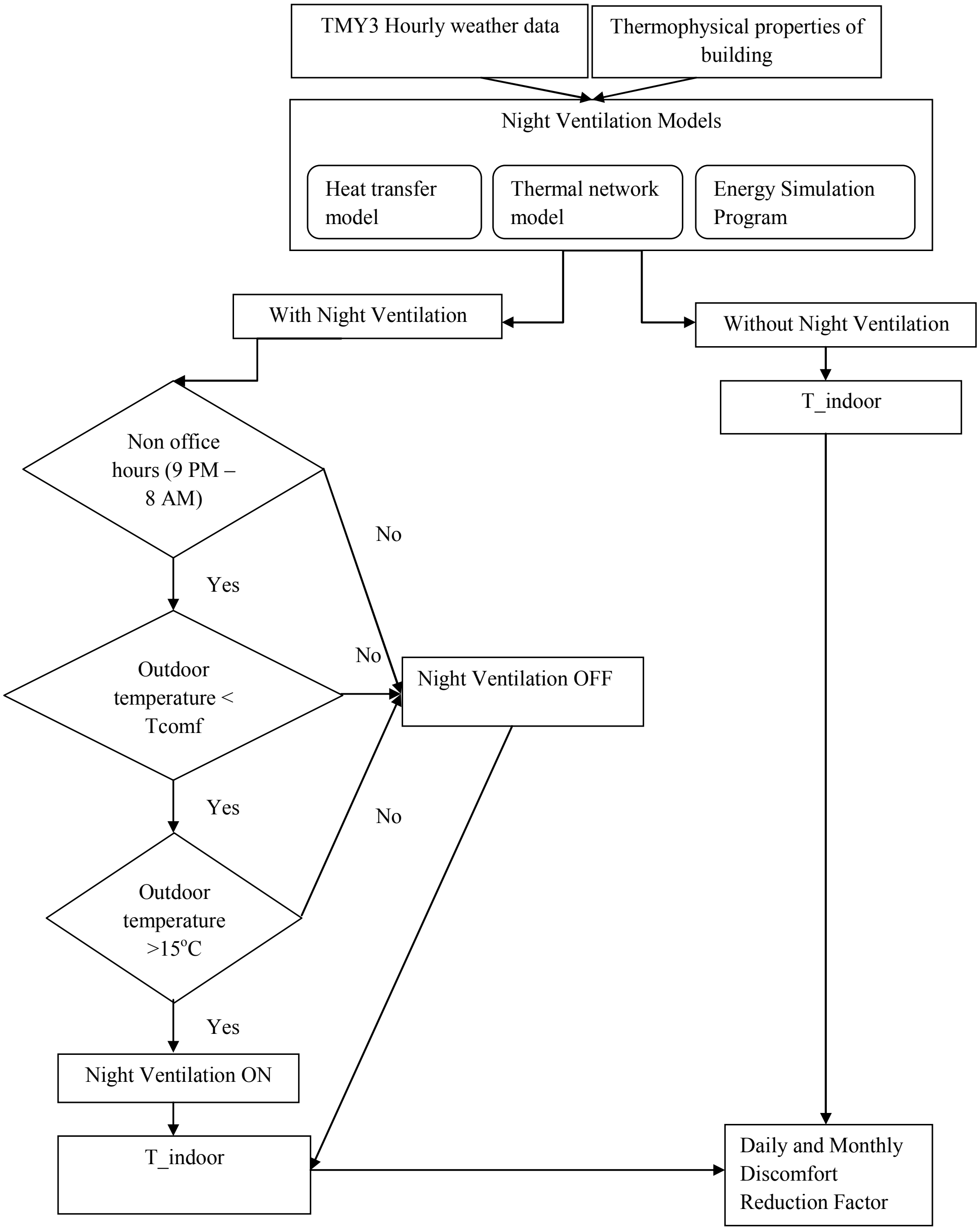

Figure 4.1 – Flow chart of simulation methodology adopted

5. MODELING - COUPLING OF THERMAL MASS AND NIGHT VENTILATION

The two models being analyzed in this research, namely the Heat Transfer model and the Thermal Network model are described, modifications made are discussed and their limitations stated.

5.1. The Heat Transfer model

Heat transfer by convection of night ventilation air at the internal thermal mass, and heat transfer occurring by convection and conduction through the building envelope are ways by which sources of different temperatures exchange heat. Heat transfer energy balance occurring among these surfaces will allow calculation of unknown parameters such as indoor air temperature. Heat transfer analysis of building envelopes can be done by different methods such as harmonic response method, Z transfer function method and response factor method. Results obtained by adopting the harmonic response method as done by Zhou et al. (2008) are used in this research.

5.1.1. Modified Zhou et al. (2008) model for night ventilation

The Zhou et al. (2008) model which accounts for coupling of thermal mass and natural ventilation in buildings has been adopted in this study dealing with night ventilation in buildings.

The parameters α_i, q, which were taken to be constant in Zhou et al. (2008) are now varied, and assume different numerical values during hours with and without night ventilation. Varying these two parameters in turn effects λ, τ and T_E which subsequently impacts average indoor temperature, damping factor and time lag which in turn influence the indoor air temperature calculation. Here after, this modified Zhou et al. (2008) is referred as the Heat Transfer model.

Zhou et al. (2008) have described six different external walls along with their thermal properties, external & interior damping factors and phase shifts. The Thermophysical properties of exterior wall of the sample structure which is a single zone space of dimensions 50ft X 50ft X 10ft (Figure 5.1), are assembled as in Table 5.1.

Table – 5.1 - Thermophysical properties of wall materials assumed in study

Material Description	**Thickness (mm)**	**K (W/ m K)**	ρ **(kg/m3)**	**C (kJ/kg K)**
Polystyrene (outside)	30	0.042	30	1.38
Foam concrete	200	0.19	500	1.05
Stucco (inside)	20	0.81	1600	1.05

This gives a heat resistance of the external wall of R_o=1.8 m^2 K/W. The eQUEST program version 3-64 was used to calculate the effective resistance value from above properties.

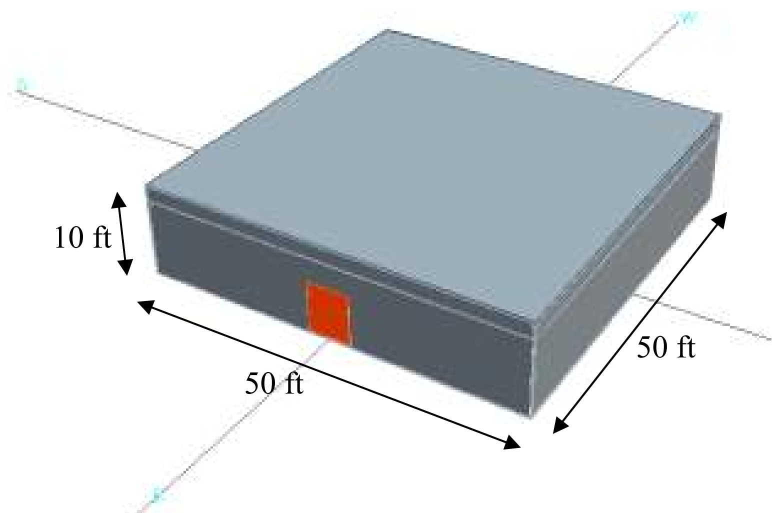

Figure 5.1 – Sample structure

Damping factor of inner surface temperature with respect to sol-air temperature, time lag of inner surface temperature with respect to sol-air temperature are 52.61 and 9.30 (h) respectively. Damping factor of inner surface temperature with respect to indoor air temperature, time lag of inner surface temperature with respect to indoor air temperature are 1.52 and 0.0193 (h) respectively. Because of the unavailability of solar air properties, solar air temperature and its amplitude of fluctuation are assumed to be same as those of outdoor air temperature.

One ACH was considered during the occupied hours. This was calculated by considering 30% additional fresh air than required by ANSI/ ASHRAE 62.1-2007, which is also the requirement of LEED BD+C (2009). To achieve a time constant of 15 hrs and 6 hrs, corresponding to one ACH, the building envelope parameters described earlier were kept constant but the interior thermal mass was altered by varying the volume of furniture. The time constant and other non dimensional terms are calculated assuming density of wood to be 600 kg/m^3 and its heat capacity to be 2.5 kJ/kg K, density of air to be 1.2 kg/m^3 and its heat capacity to be 1.005 kJ/kg K. A heat transfer coefficient of 8.29 W/m^2K corresponding to 3 ACH (Zhou et al., 2008) is taken as appropriate. Using Equation 5.1 from Kreider et al., (2005) relates convective heat transfer coefficient (α_i) with velocity of flow over smooth surfaces results in α_i being proportional to velocity or ACH to be power of 0.8.

$$\alpha_i = 6.2(\frac{v^4}{L})^{\left(\frac{1}{5}\right)} \quad (5.1)$$

where

v is the indoor air velocity in meters/second

and L is the length of plane or the wall surface in meters.

A volume of 8 m^3 of furniture was required to achieve a time constant of 15 hrs for one ACH and it has been reduced to 2.85 m^3 to achieve a time constant of 6 hrs for one ACH. Table 5.2 corresponding to 15 hrs of time constant for one ACH, assembles values of various parameters appearing in the model for different ACH values.

Table 5.2 – Values of the Heat Transfer model parameters for increasing values of air changes per hour

ACH	q	αi	λ	τ	a	b	c	d	ξi	fi
0.50	0.10	1.98	6.97	30.09	3.38	7.90	-0.90	0.09	4.82	0.11
1.00	0.20	3.44	6.07	15.04	3.07	3.96	-0.91	0.07	3.79	0.18
2.00	0.39	5.99	5.28	7.52	2.81	1.99	-0.92	0.06	2.62	0.27
3.00	0.59	8.29	4.87	5.01	2.66	1.33	-0.93	0.06	2.01	0.31
4.00	0.79	10.44	4.60	3.76	2.57	1.00	-0.93	0.06	1.65	0.34
5.00	0.98	12.47	4.40	3.01	2.50	0.80	-0.94	0.05	1.40	0.36
6.00	1.18	14.43	4.24	2.51	2.45	0.67	-0.94	0.05	1.23	0.37
7.00	1.38	16.33	4.11	2.15	2.40	0.58	-0.94	0.05	1.10	0.38
8.00	1.57	18.17	4.00	1.88	2.37	0.51	-0.94	0.05	1.00	0.39
9.00	1.77	19.96	3.91	1.67	2.34	0.45	-0.94	0.05	0.92	0.40
10.00	1.97	21.72	3.83	1.50	2.31	0.41	-0.94	0.05	0.86	0.40

As stated earlier, night ventilation is implemented only during non office hours and when outdoor temperatures are below comfort temperatures and greater than 15 ^{o}C. To exclude days which can result in overcooling of the structure, only days with a maximum temperature in a day greater than 18 ^{o}C are considered during the estimation of Daily Discomfort Reduction Factor. Figure 5.2 depicts a plot of the diurnal indoor temperature profile with night ventilation for time constants of 15 hrs & 6 hrs using the Heat Transfer model, another plot without night ventilation and a third plot of ambient temperature for two days when night ventilation is effective for Phoenix, AZ.

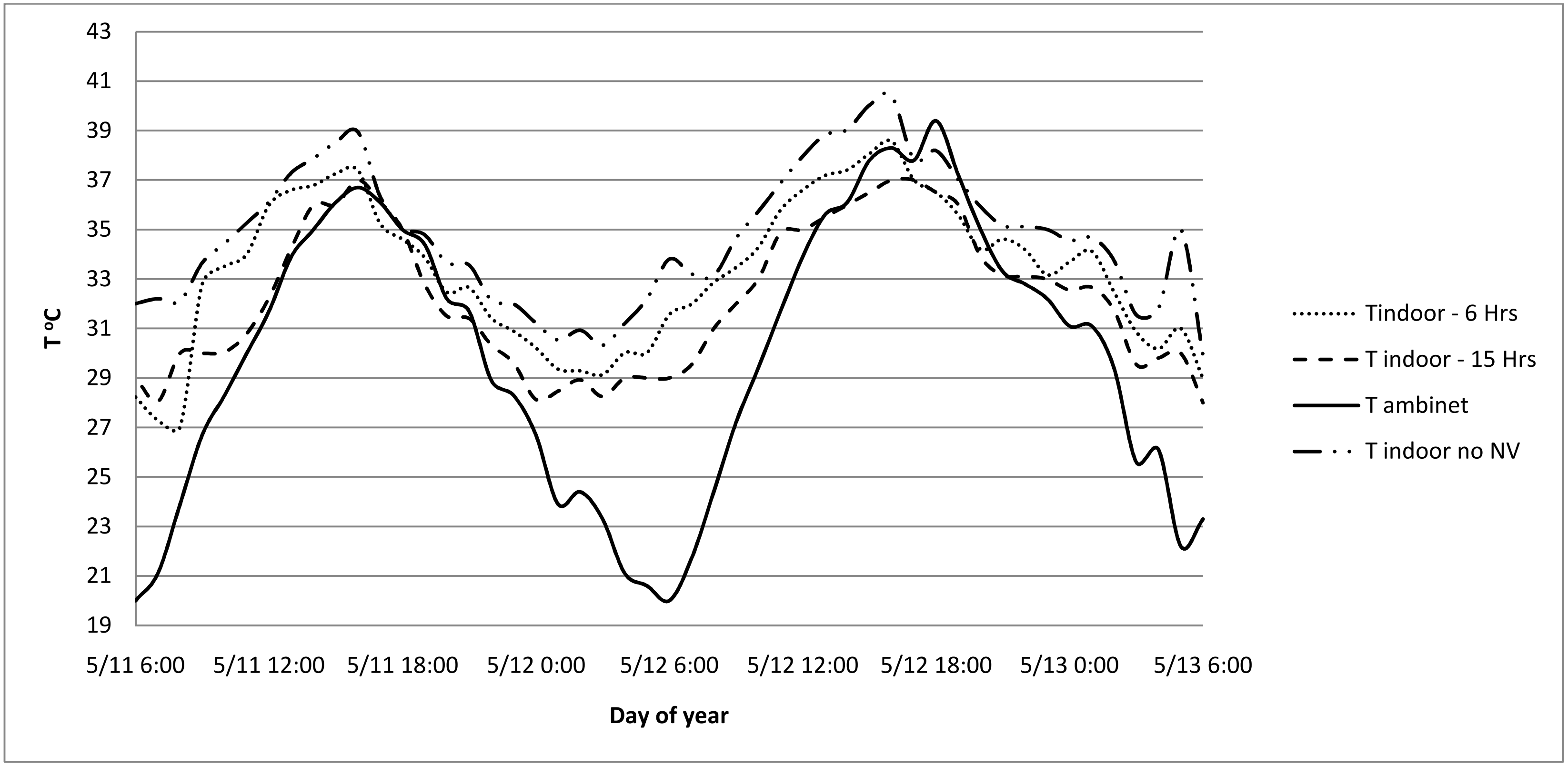

Figure 5.2 – Diurnal temperature profiles from 5/11 6 AM to 5/13 6 AM from Phoenix, AZ with the indoor temperatures calculated using the Heat Transfer model

5.1.2. Limitations

The temperature distribution of the internal thermal mass is assumed to be uniform and equal to the indoor air temperature. This may not be the case in actual situations. There will be a time delay for the thermal mass to reach its steady state value, which will be same as the temperature of indoor air. All heat gain in the building is assumed lumped, i.e. treated considered as a single heat source. The distribution of heat gain may affect the distribution of the indoor air temperatures. This model is therefore a simplified one as compared to actuality. This simplified model may affect the accuracy in predicting the indoor temperature profile and the discomfort reduction factor, and hence, will only provide indications of generalized trends.

5.2. The Thermal Network model

Thermal network models are electrical network approximations of thermal dynamic behavior of buildings. Heat transfer coefficients are reciprocals of the electrical resistances and thermal capacitances are similar to electrical capacitors. Electrical laws can be used to solve these thermal networks. Under the thermal network approach, one approximates a building as being composed of a finite number of elements, called nodes, each of which is assumed to be isothermal. To model heat exchange, the nodes are connected by resistances, thus forming a thermal network. Even though the thermal network also referred to as RC (Resistance and Capacitance) network, is a crude approximation of thermal flows in buildings, it gives the designer a simple tool for estimating the warm-up and cool down times of building structures.

5.2.1. Modified Feuermann and Hawthorne model (1991)

The RC network assumed by Feuermann and Hawthorne (1991) in their study of the potential and effectiveness of passive night ventilation cooling, has been modified to the one shown in Figure 5.3.

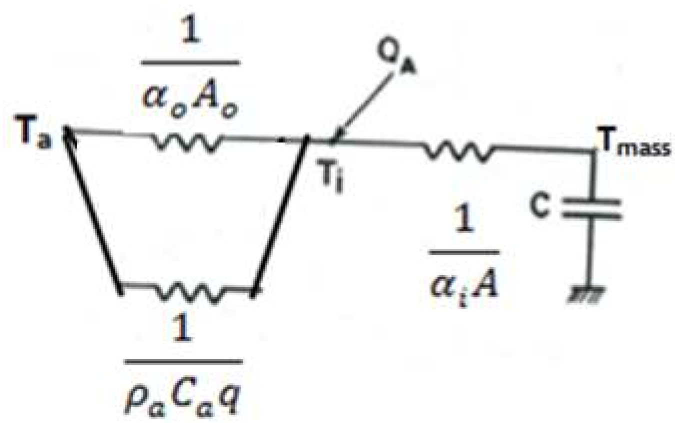

Figure 5.3 The Thermal Network model

Note that R_1 is the effective resistance made up of two resistances in parallel $\frac{1}{\alpha_o A_o}$ and $\frac{1}{\rho_a C_a q}$ and the another resistance in series, namely $R_2 = \frac{1}{\alpha_i A}$.

The thermal network in Figure 5.3 was solved to determine Ti in terms of other parameters by using equation 3.6 developed by Reddy (1989). A small difference is that solar gains have been neglected. The proposed model differs from the Feuermann and Hawthorne (1991) model by considering the variability in comfort temperatures in accordance to ASHRAE Standard 55-2004. This modified model hereafter is referred to as Thermal Network model.

Table 5.3 specifies the volumetric air flow and interior convective heat transfer coefficient for scenarios with and without night ventilation and for different ACH values. The values of ACH and convective hear transfer coefficients are assumed in accordance with section 5.1.2.

Table 5.3 – Air changes per hour (ACH) and convective heat transfer coefficients during day time and night time for scenarios with and without night ventilation

		ACH	**q** (m^3/sec)	α**i (**(W/m^2 K))
With Night Ventilation	**Night**	10	1.97	12
	Day	1	0.2	7.22
Without Night Ventilation	**Night**	0.5	0.1	6
	Day	1	0.2	7.22

The time constant, which is defined as time taken for a response to attain 1/e ~0.368 of its final steady state when subject to a change in the forcing function is calculated by maintaining constant loads in the building and step changing the forcing function (outdoor temperature) by an abrupt step change. The time taken for the response function (indoor temperature) to reach to 36.8% of its asymptote value is calculated. Figure 5.4 is the plot of response function (indoor temperature) with respect to time in minutes. It can be noticed that indoor temperature exhibits an asymptotic behavior with the time taken to reach 36.8% of its asymptote value in 360 minutes (6 hrs). This was achieved when internal capacitance is set to 87,500,000 J/ °C (24.30 kWh/ °C). Similarly 15 hrs and 25 hrs time constants were achieved for internal capacitances of 60.26 kWh/ °C and 88 kWh/ °C respectively. Figure 5.5 assembles plots of the diurnal indoor temperature profiles generated using the Thermal Network model with night ventilation for time constants of 15 hrs & 6 hrs, plot of indoor temperature without night ventilation and ambient temperature for two days in Phoenix, AZ.

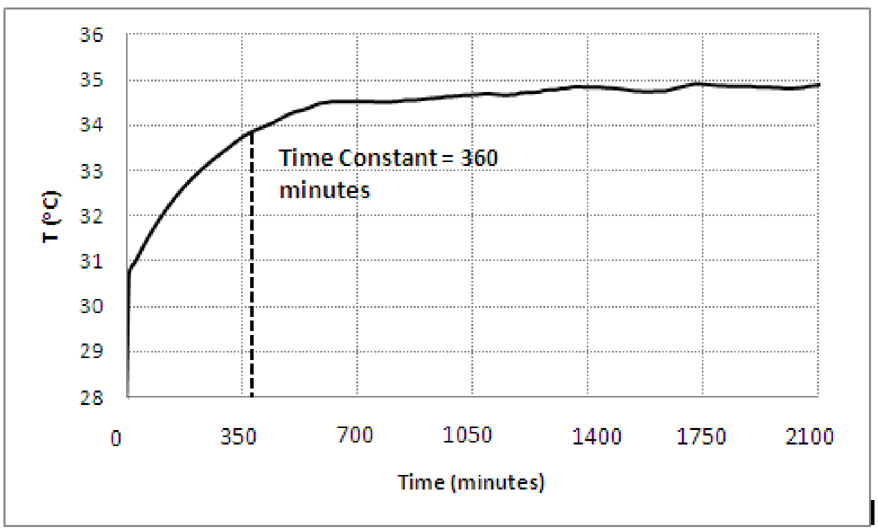

Figure 5.4 – Plot of response function (indoor temperature) for increasing time period (minutes) to estimate time constant of the building in the Thermal Network model.

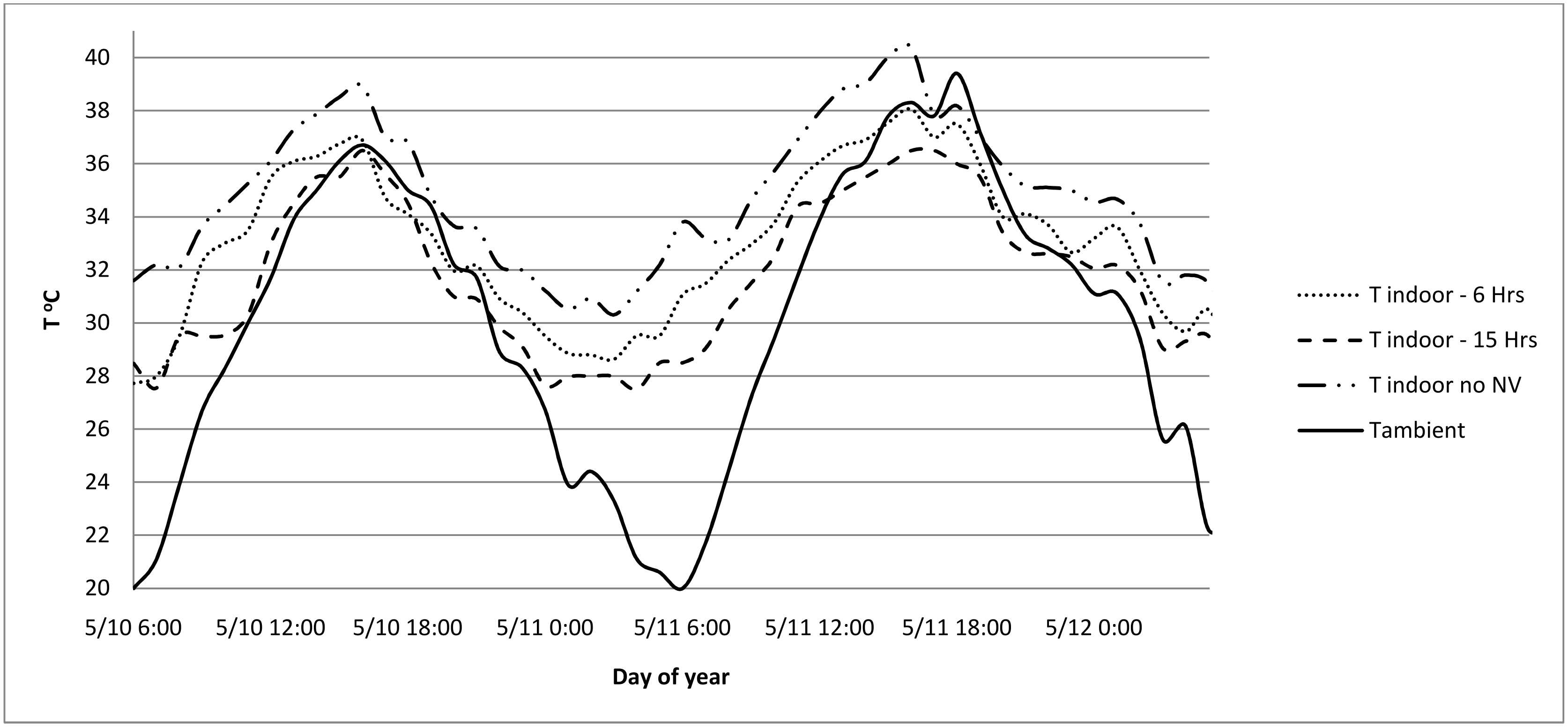

Figure 5.5 – Diurnal temperature profiles for two days in Phoenix, AZ with the indoor temperatures calculated using the Thermal Network model

5.2.2. Limitations

The Thermal Network model is a simple approximation of the dynamic behavior of a building structure subject to night ventilation and incorporates several limiting assumptions. The interaction between thermal mass and ventilated air is simplified. Since the thermal capacity of the building is approximated by a single capacitance, its sensitivity to thermal mass behavior may be improperly captured. The effect of solar heat gains has not been considered. All heat gain in the building is lumped and considered as a single heat source. The distribution of heat gain may affect the distribution of indoor air temperature. This simplified model may affect the accuracy in predicting the indoor temperature profile and in computing the discomfort reduction factor.

6. ANALYSIS OF MODELS

6.1. Effect of location – Phoenix, AZ and Albuquerque, NM

To observe the effect of weather data on night ventilation, indoor temperature dynamics can be simulated from which DRF for daily & monthly time scales and for two locations, Phoenix, AZ and Albuquerque, NM using the TMY3 weather data can be determined.

Figures 6.1 and 6.2 are plots of daily & monthly DRFs for Phoenix, AZ and Albuquerque, NM respectively, obtained using heat transfer model.

Figure 6.3 and 6.4 are the plots of daily & monthly DRFs for Phoenix, AZ and Albuquerque, NM respectively, obtained using thermal network model assuming a 15 hr time constant.

From Figures 6.1 and 6.3, it can be observed that for Phoenix, AZ night ventilation will be effective from January to April and October to December. This is consistent in both the heat transfer model and the thermal network model. These are the months with relatively lower peak temperatures and larger swings in temperature. This is in agreement with Givoni (1994) who stated that night ventilation is applicable to regions/ seasons where daytime temperatures are between 30 ^{o}C and 36 ^{o}C and the night temperatures are below 20 ^{o}C. Figure 6.5 is a plot of peak daily temperatures and temperature swings in ambient temperature for Phoenix, AZ using the TYM3 data. From the plot it can be noticed that periods from January to April and October to December have lower peak temperatures (less than 36 ^{o}C) and relatively larger temperature swings. The Discomfort Reduction Factor (DRF) is largest during the months of March and November with a value of 0.40 using Heat Transfer model. However, the largest DRF is 0.48 in March and 0.41 in November using Thermal Network model. This discrepancy in DRF values between the Heat Transfer and the Thermal Network models is explained in Section 6.3.

From Figures 6.2 and 6.4, it can be observed that, in Albuquerque, NM, night ventilation is effective from April to October, which is different from that in Phoenix, AZ. This behavior of night ventilation effectiveness in Albuquerque, NM, can be understood from Figure 6.6, which shows plots of daily peaks and swings in ambient temperature at Albuquerque, NM using

TMY3 data. Beyond the months of April to October, the daily peak temperatures are very cold and night ventilation is not an effective strategy. During April to October, most of the daily peak temperatures are below 36 ^{o}C and temperature swings are relatively larger. Between April to October, DRF values are largest during months of May, September and October and lowest during June and July. Similar patterns are observed in both the Heat Transfer model and the Thermal Network model predictions.

For buildings, generally office buildings, which are only occupied during certain periods of day, the calculation of DRFs should be done only for hours when the building is occupied. Figure 6.7 is the plot for comparison of monthly DRFs calculated only from 9 AM to 9 PM and over 24 hour period for Phoenix, AZ using the Heat Transfer model for a building with time constant of 15 Hrs. From Figure 6.7 it can be noticed that both plots are quite close, with a slight decrease in DRFs (max is less than 8%) for the case of occupancy assumed between 9 AM to 9 PM. This is due to the fact that, benefits of night ventilation are accounted for 24 hour time periods even during non-occupancy hours when DRFs are calculated over 24 hour time periods.

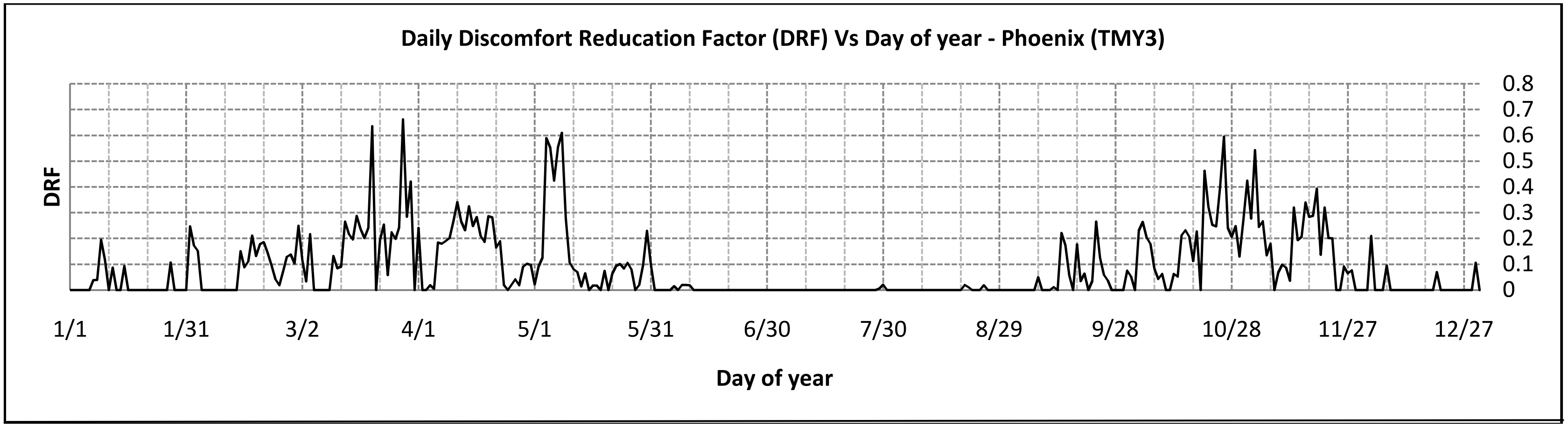

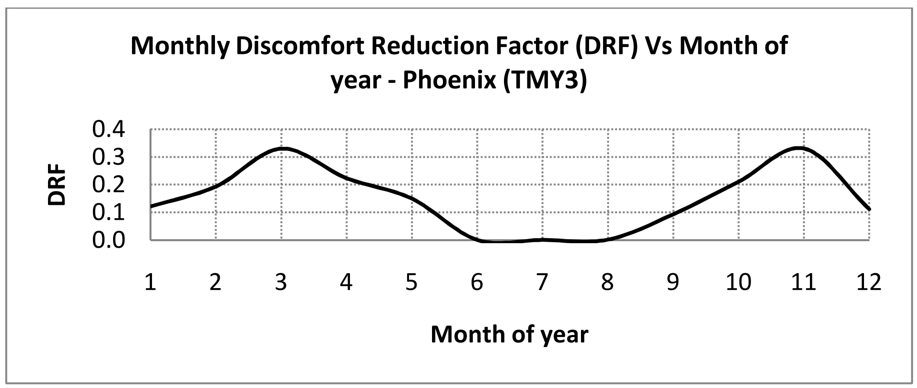

Figure 6.1 – Daily and Monthly Discomfort Reduction Factors for Phoenix, AZ using the Heat Transfer model with time constant of 15 hrs

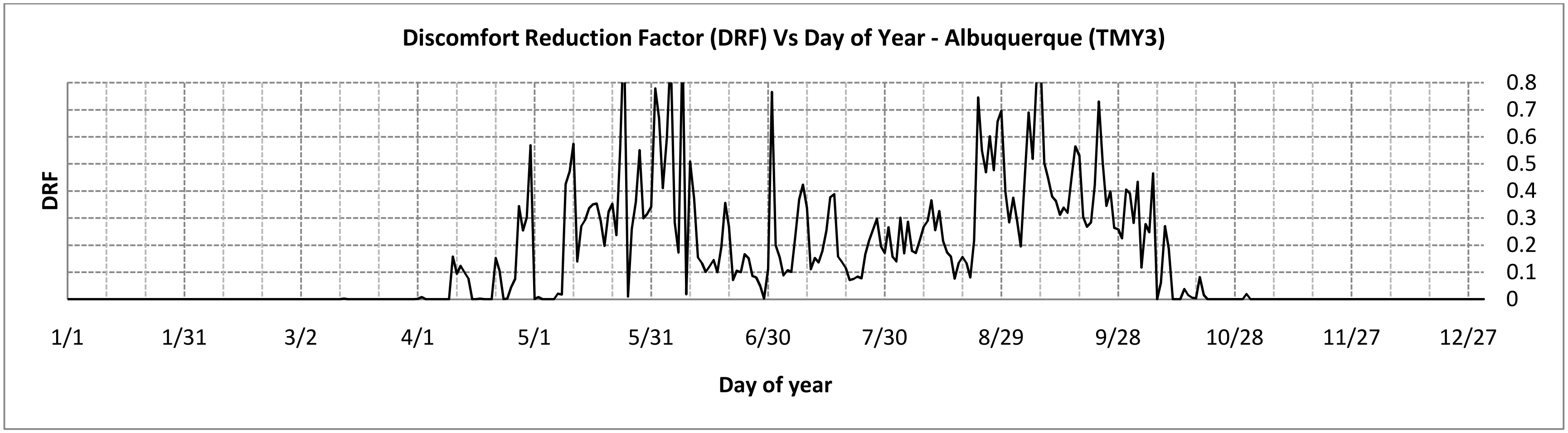

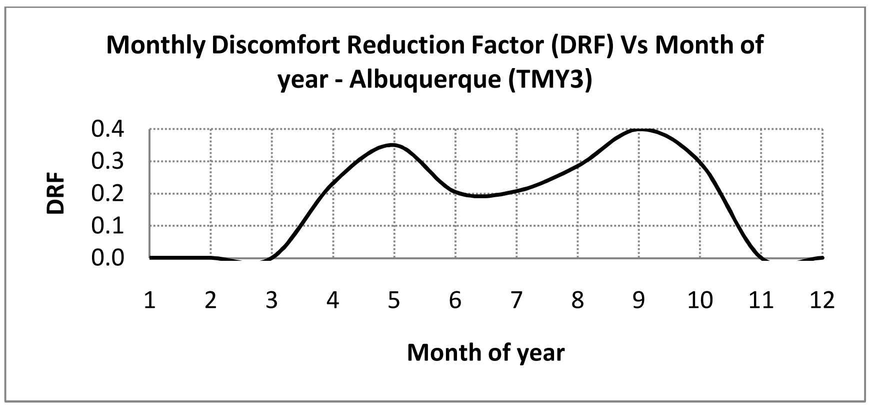

Figure 6.2 – Daily and Monthly Discomfort Reduction Factors for Albuquerque, NM using the Heat Transfer model with time constant of 15 hrs

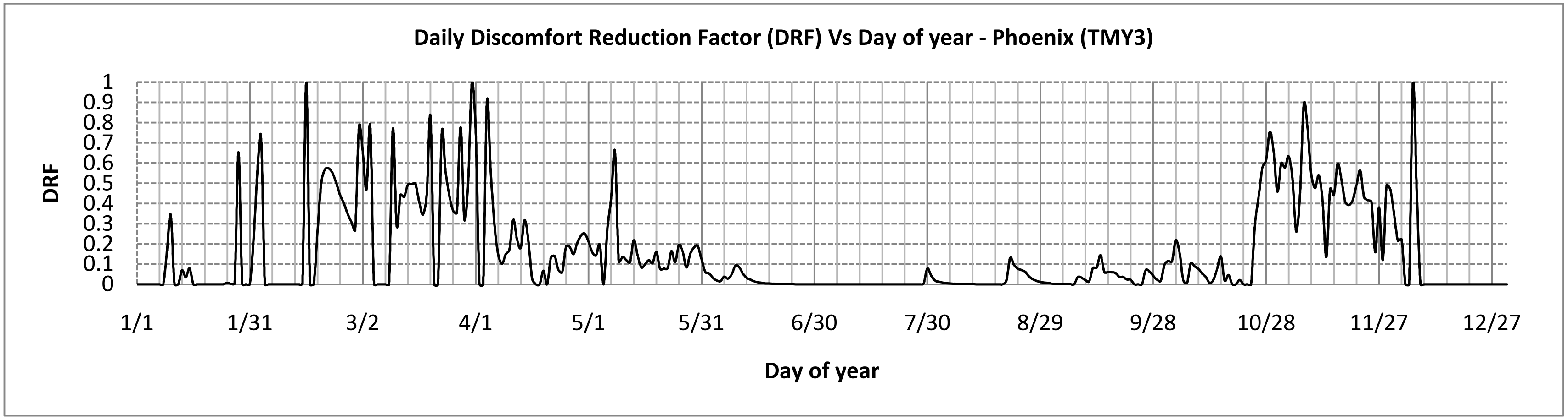

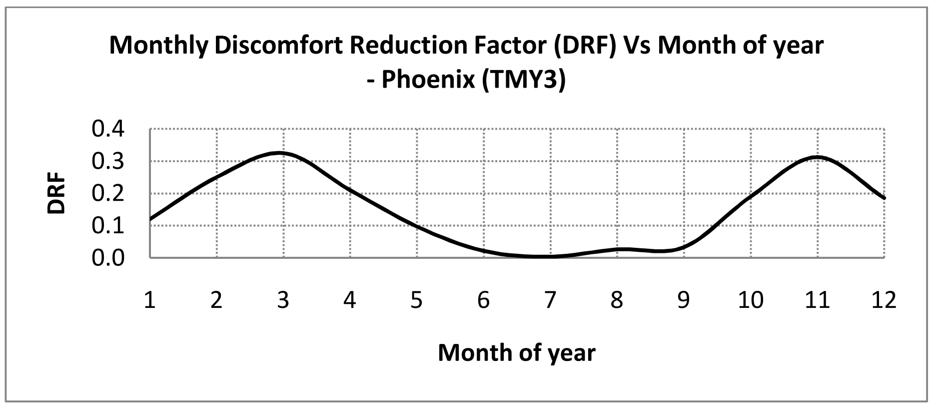

Figure 6.3 – Daily and Monthly Discomfort Reduction Factors for Phoenix, AZ using the Thermal Network model with time constant of 15 hrs

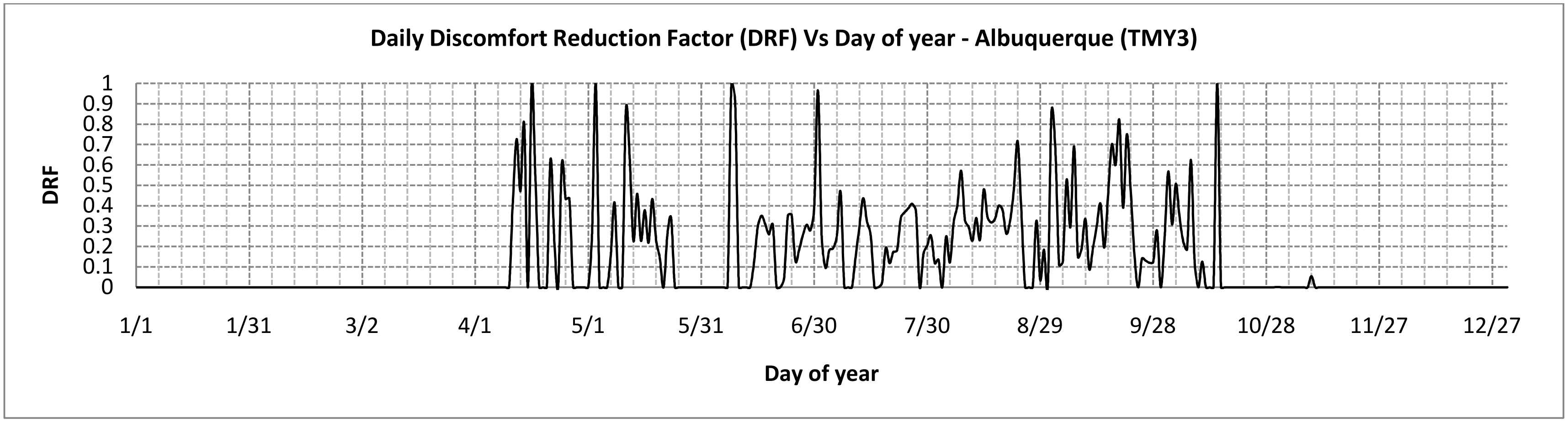

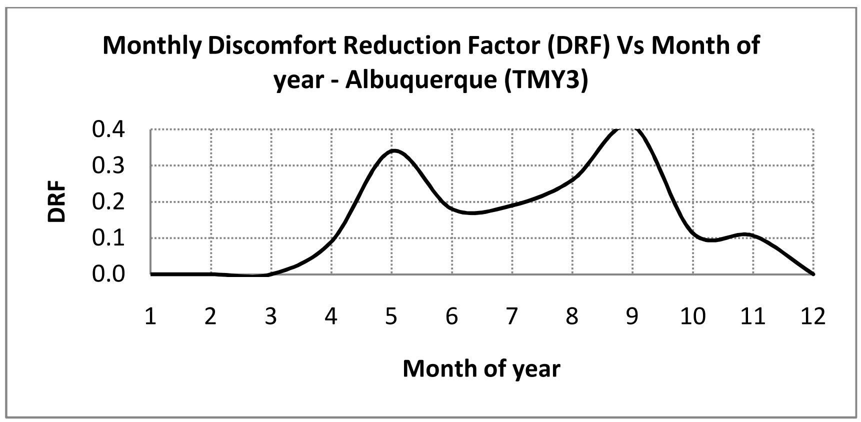

Figure 6.4 – Daily and Monthly Discomfort Reduction Factors for Albuquerque, NM using the Thermal Network model with time constant of 15 hrs

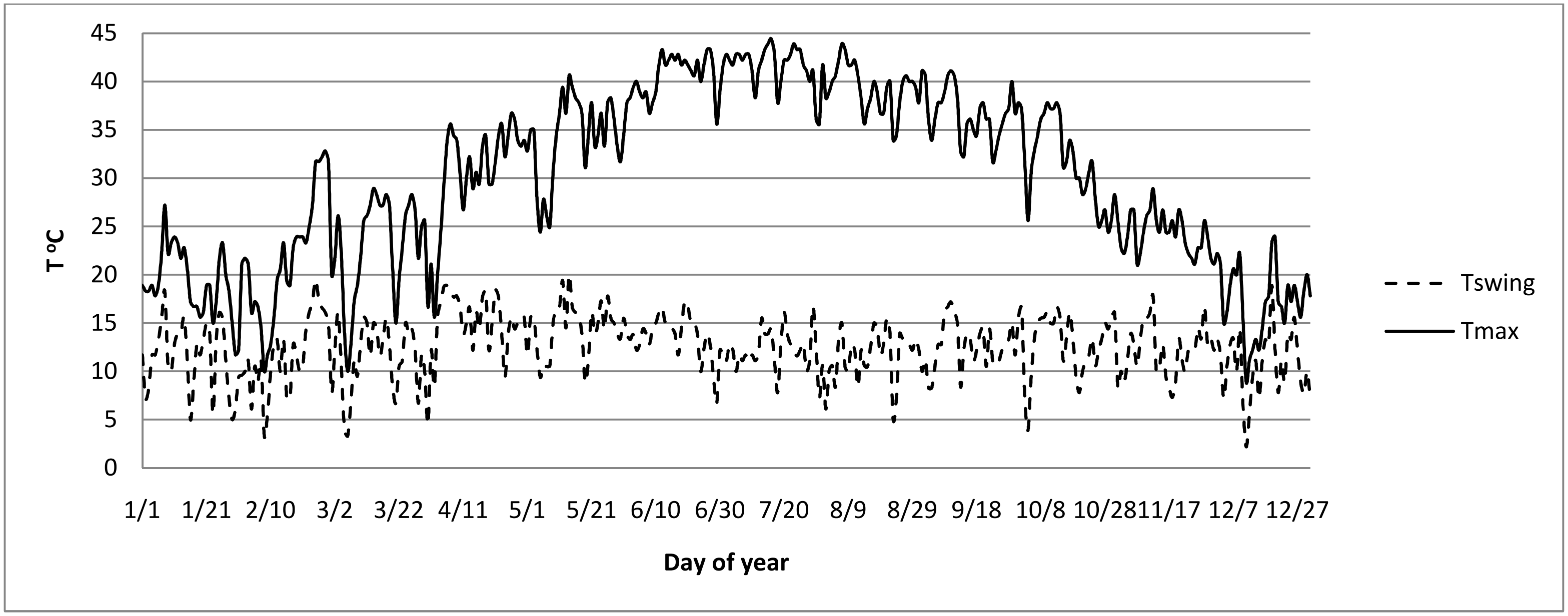

Figure 6.5 – Variation in daily peaks and swing in ambient temperature for a whole year in Phoenix, AZ using TMY3 data

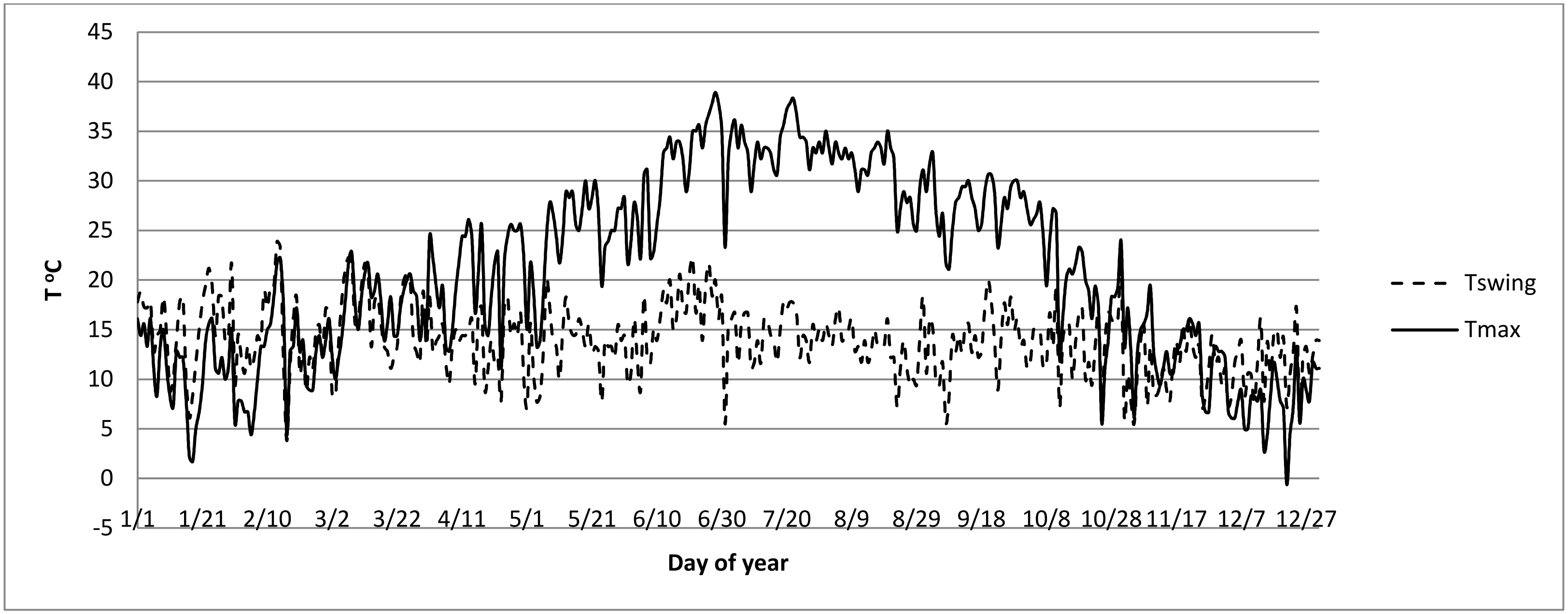

Figure 6.6 – Variation in daily peaks and swing in ambient temperature for a whole year in Albuquerque, NM using TMY3 data

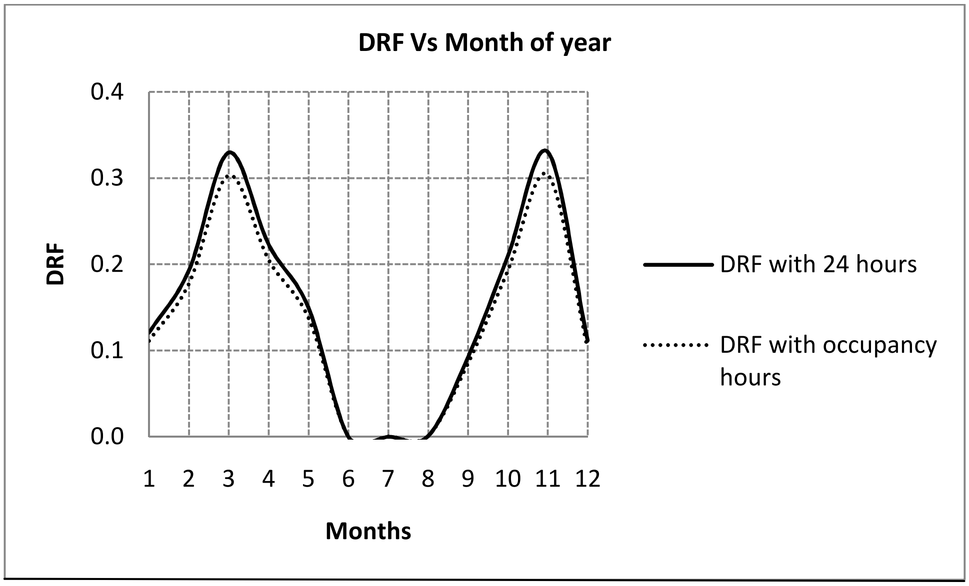

Figure 6.7 - Comparison of monthly DRFs calculated assuming occupancy hours (9 AM to 9 PM) and for 24 hour period. Phoenix, AZ with the Heat Transfer model used to simulate building dynamics with time constant of 15 hrs

6.2. Effect of time constant – 25 hrs, 15.5 hrs and 6 hrs

Time constant is defined as time taken for a response to attain 1/e ~0.368 of its final steady state value when subject to a step change in the forcing function. The longer the time constant of a building, the longer it takes to cool down or warm up the building structure. Thus, time constant is reflective of the thermal capacity of the building. Thermal capacity of the building plays a significant role in night ventilation. When the building is ventilated at night, its cooling capacity increases with increase of thermal capacity or time constant, so that this cooled mass can delay the increase of indoor temperature for the next day. Three time constants of 25 hrs, 15.5 hrs and 6 hrs were used to test the effectiveness of night ventilations. These time constants were achieved by varying the capacitance of internal thermal mass.

Figures 6.8 and 6.9 are plots of Monthly DRFs for time constant of 25 hrs, 15 hrs and 6 hrs for Phoenix, AZ and Albuquerque, NM, respectively calculated using the Heat Transfer model.

Figures 6.10 and 6.11 are the plots of Monthly DRFs for time constant of 25 hrs, 15 hrs and 6 hrs for Phoenix, AZ and Albuquerque, NM, respectively calculated using the Thermal Network model.

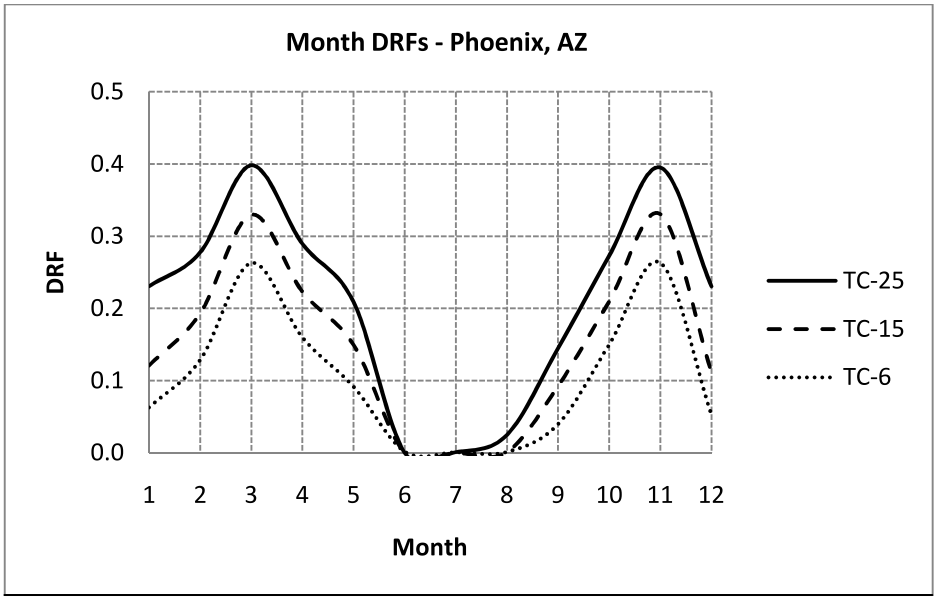

Figure 6.8 – Monthly DRFs for Time Constant (TC) of 25 hrs, 15 hrs and 6 hrs for Phoenix, AZ using the Heat Transfer model

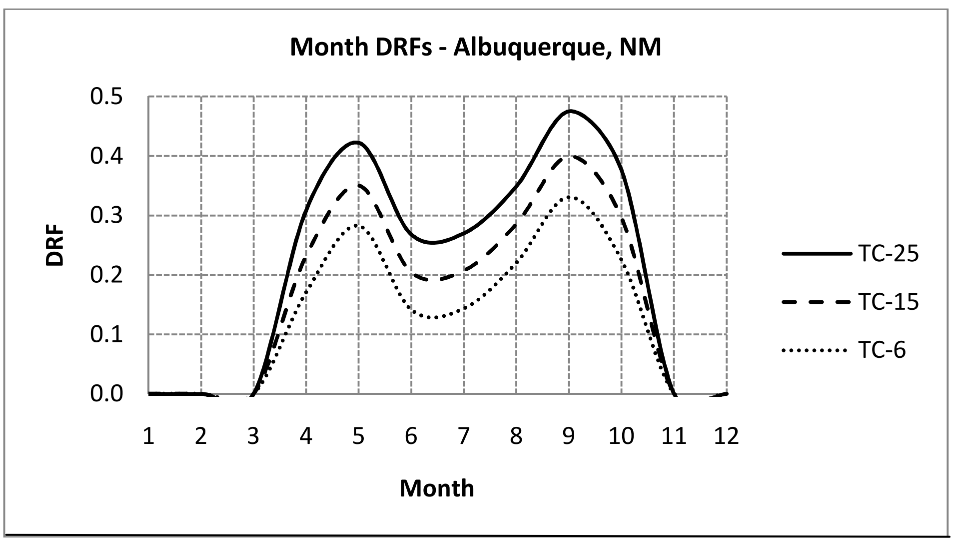

Figure 6.9 – Monthly DRFs for Time Constant (TC) of 25 hrs. 15 hrs and 6 hrs for Albuquerque, NM using the Heat Transfer model

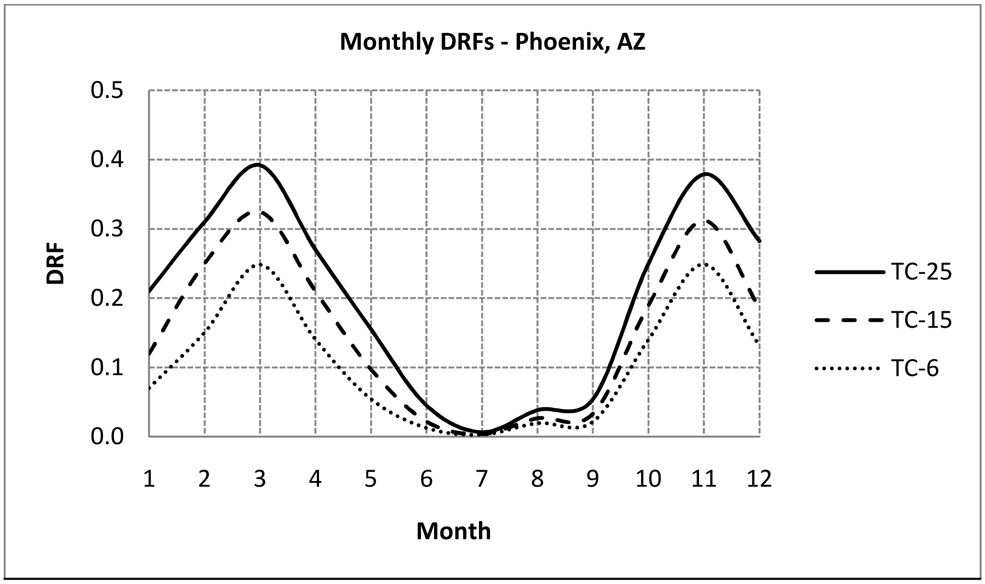

Figure 6.10 – Monthly DRFs for Time Constant (TC) of 25 hrs, 15 hrs and 6 hrs for Phoenix, AZ using the Thermal Network model

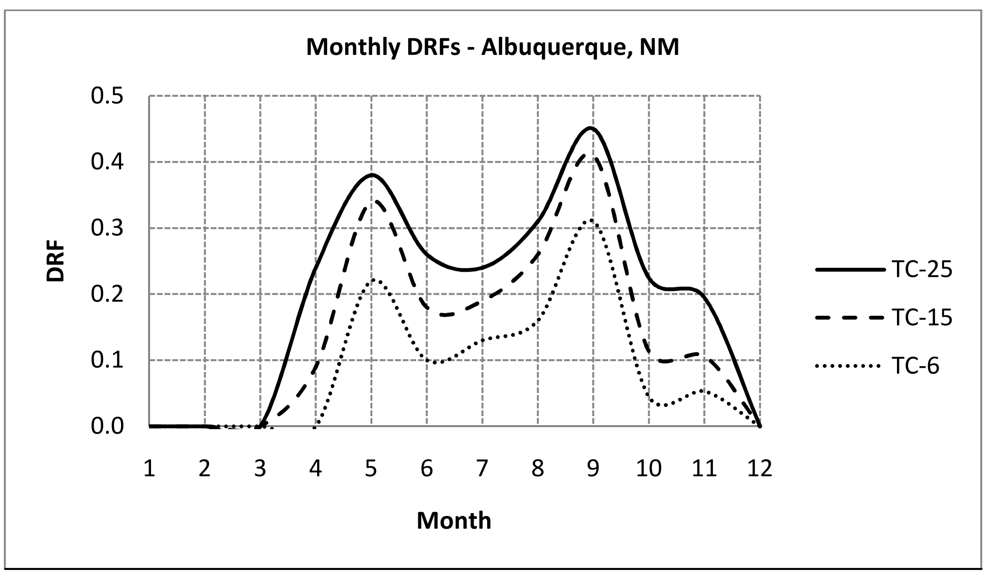

Figure 6.11 – Monthly DRFs for Time Constant (TC) of 25 hrs, 15 hrs and 6 hrs for Albuquerque, NM using the Thermal Network model

From Figures 6.8 through 6.11, it can be observed that irrespective of the geographic location, buildings with higher time constants are more attractive for implementing the night ventilation strategy as compared to one with lower time constants since their DRFs are higher. Higher time constants signify larger thermal capacity; these buildings can better hold the "cold" during the nights and release it when the space tries to warm up the next day. This property will delay the increase in the indoor temperatures with respect to outdoor temperatures. Also, it can be noticed that sensitivity to time constant is greater in Phoenix, AZ in both the models. However, there is a variation in sensitivity levels among the model, and this is discussed in Section 6.4. In Heat Transfer models, the difference between both model predictions in peak DRF values for Phoenix, AZ is 10% whereas for Albuquerque, NM it is 4%. Further research could be directed to finding the relation between ambient weather and sensitivity of time constant; the sensitivity to time constant on DRF values may also decrease with higher values of time constant.

6.3. Effect of ACH – 20, 10 and 5

Air Changes per Hour (ACH) is a measure of how many times the air within a defined space (normally a room or house) is replaced with outdoor air. In this study, the peak ACH considered during the operating hours of night ventilation is varied and its effect on DRFs is observed. Peak ACH of 20, 10 and 5 are assumed for both climate locations of Phoenix, AZ and Albuquerque, NM using both the Heat Transfer the Thermal Network models. The monthly DRF values are shown in Figures 6.12 to 6.15. We note that DRFs increase as ACH increases. However, it is observed that the increase in DRF by increasing ACH is not as pronounced as that when the time constant is increased.

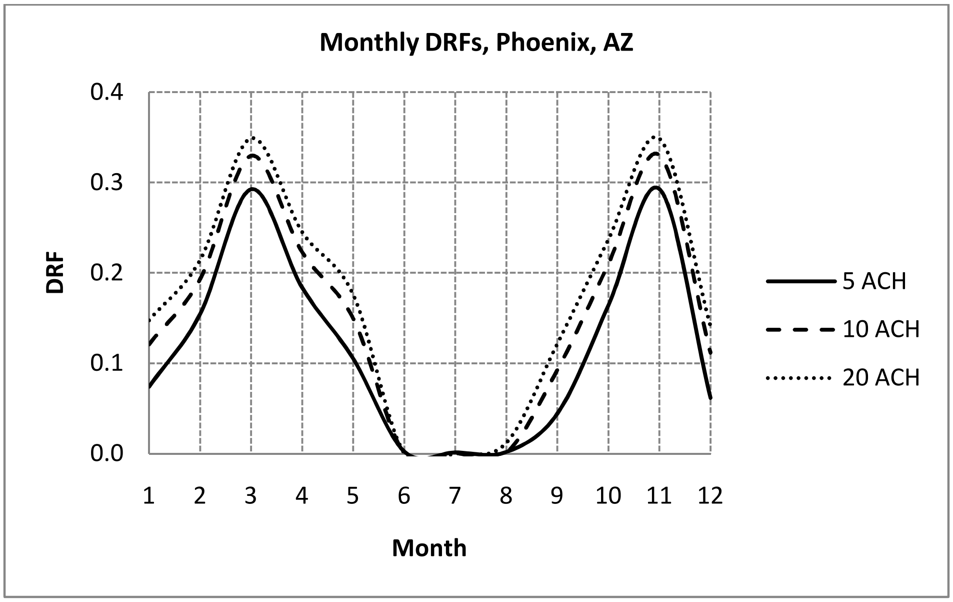

Figure 6.12 – Monthly DRFs for peak ACH of 5, 10 and 20 for Phoenix, AZ using the Heat Transfer model

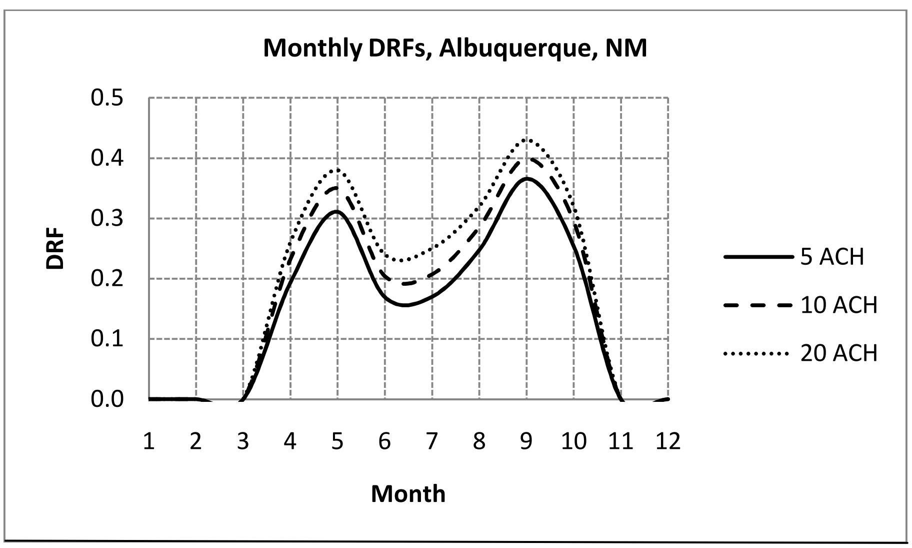

Figure 6.13 – Monthly DRFs for peak ACH of 5, 10 and 20 for Albuquerque, NM using the Heat Transfer model

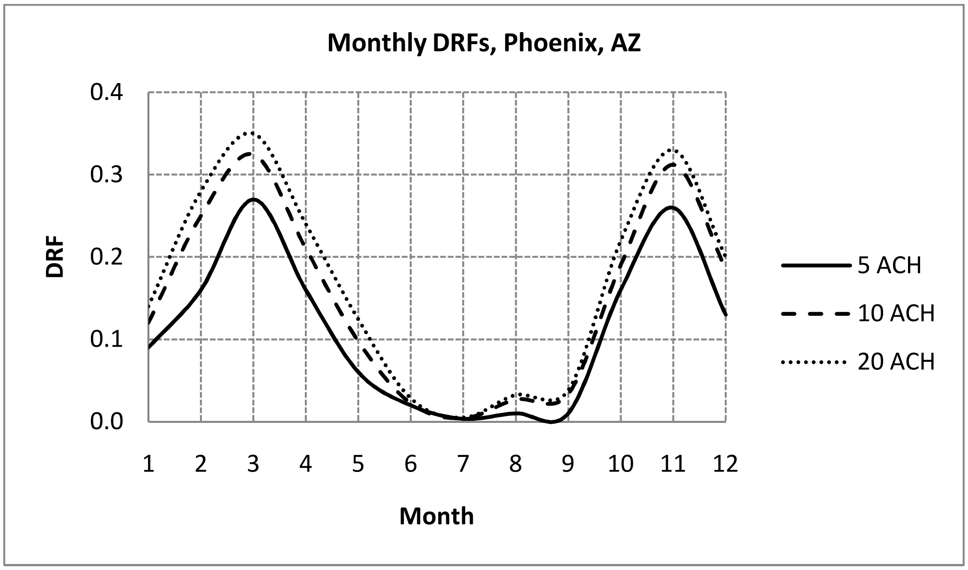

Figure 6.14 – Monthly DRFs for peak ACH of 5, 10 and 20 for Phoenix, AZ using the Thermal Network model

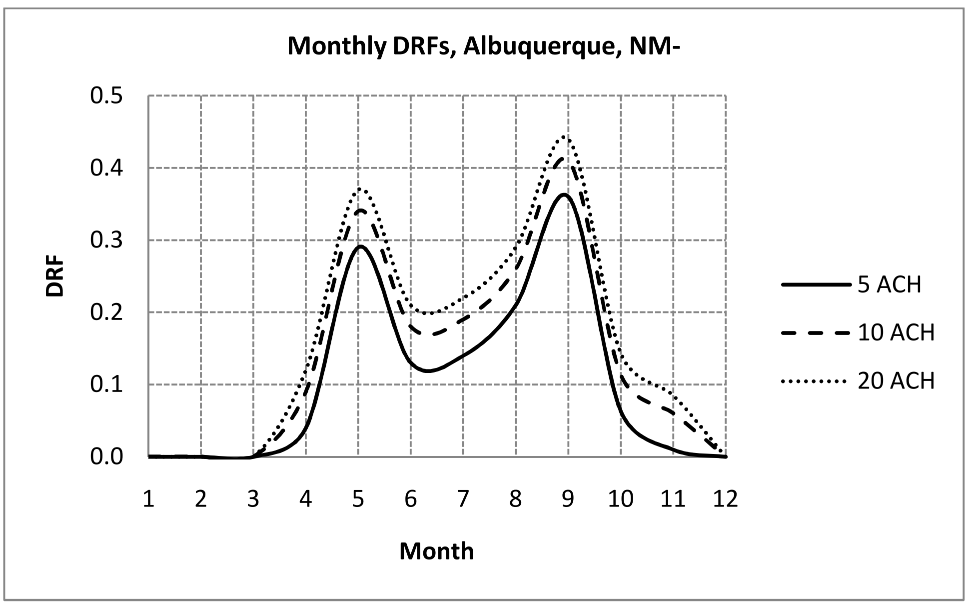

Figure 6.15 – Monthly DRFs for peak ACH of 5, 10 and 20 for Albuquerque, NM using the Thermal Network model

6.4. Comparison of the Heat Transfer and the Thermal Network models

Comparing Figure 3.4, which is the thermal network approximation of the Heat Transfer model and Figure 5.3 which is the Thermal Network model, it can be noted that they are similar except for resistance ($\frac{1}{\rho_a c_a q}$). This factor accounts for the capacity of ventilation air and is coupled differently in either model it is in parallel to all other resistors in the Heat Transfer model whereas, it is taken to be coupled in parallel to the conduction & convection resistance of the exterior envelope and in series with the convective resistance of the internal thermal mass. Ascertaining which is more realistic would probably depend on the specific building. Also, the Heat Transfer model is a closed form solution while the Thermal Network model is solved using numeric methods.

Discomfort Reduction Factors (DRFs) have been calculated following both models for both locations. Figures 6.16 and 6.17 indicate that there is a difference in the monthly DRF values though, the patterns are quite similar. The variation in DRF values is due to the difference in how the coupling of thermal mass and night ventilation in buildings is approximated in both models.

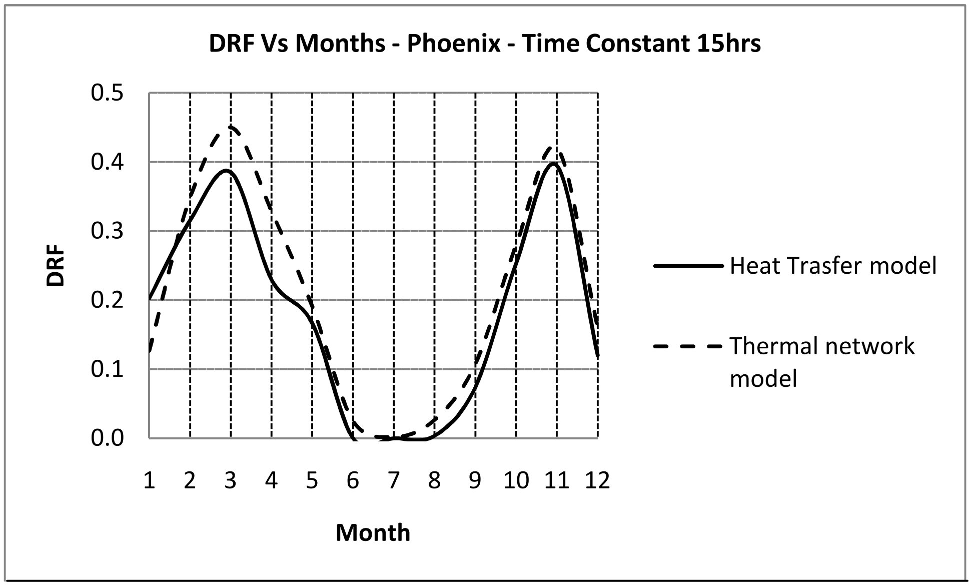

6.16 – Comparison of variability in DRFs following the Heat Transfer model and the Thermal Network model for Phoenix, AZ for a time constant of 15 hrs and peak ACH of 10

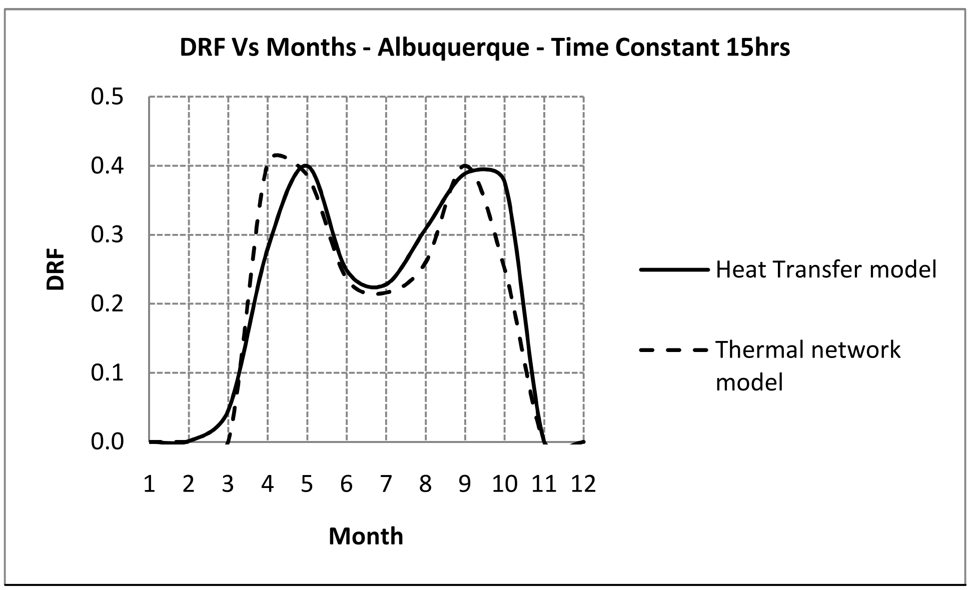

6.17 – Comparison of variability in DRFs following the Heat Transfer model and the Thermal Network model for Albuquerque, NM for a time constant of 15 hrs and ACH of 10

6.5. Comparison with results from whole building energy simulation model

Whole building energy simulation models are comprehensive mathematical models to evaluate the energy performance of buildings. eQUEST, one of the available energy simulation tools, was designed to allow users to perform detailed analysis of current state-of-the-art building design technologies. It is a very sophisticated building energy simulation program which however, does not require extensive experience in the art of building performance modeling. The simulation engine within eQUEST is derived from the latest official version of DOE-2.

The sample building with properties listed in Table 5.1 and ventilation volumes shown in Table 5.3 was simulated using eQUEST for Phoenix, AZ, with TMY3 data. The indoor temperature profiles for scenarios with and without night ventilation were generated from which daily and monthly DRFs were calculated using equations 4.1 and 4.2. As shown in Figure 6.18., it can be noticed that the pattern followed by monthly DRFs is similar to the one followed by both models. Time constant of this model was estimated by the method discussed in section 5.2.1. By maintaining constant loads in the building and changing the forcing function (outdoor temperature) in a step-wise manner, the time taken for the response function (indoor temperature) to attain 36.8% of its final steady state value is calculated. Figure 6.19 is the plot of response function (indoor temperature) with respect to time elapsed in minutes. It can be noticed that indoor temperature has reached a near asymptote at around 80 ^{o}F,

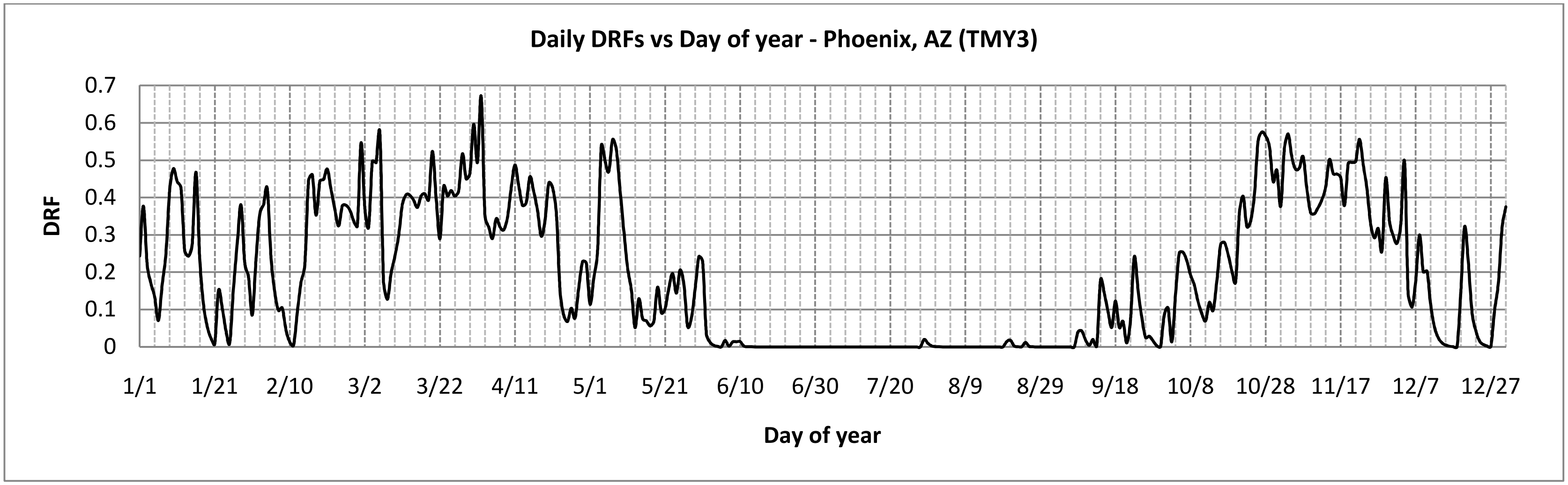

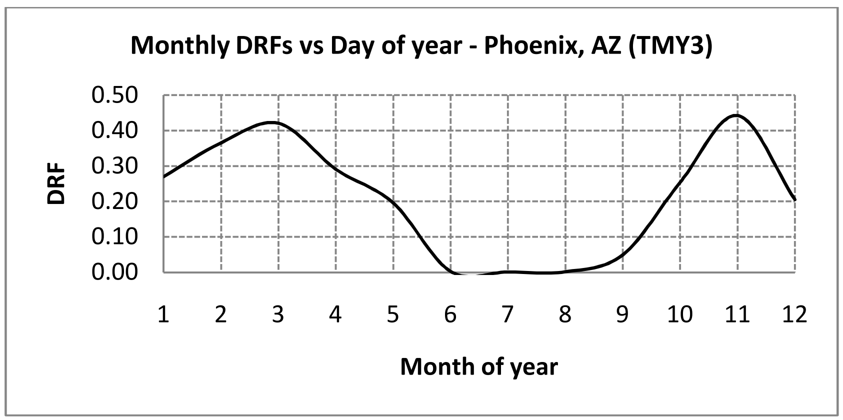

Figure - 6.18 – Daily and Monthly Discomfort Reduction Factors for Phoenix, AZ using eQUEST program from an initial value of around 86 °F. Thus the time constant of the sample structure chosen is estimated to be 26.8 hrs. DRFs of this structure are similar to DRFs achieved for a time constant of 25 hrs using the Heat Transfer model and the Thermal Network model. The time constant of the building can be varied using eQUEST 3.64 (2010) generally in three ways, custom or standard weighting factor, internal mass or custom weighting factor and by including internal walls with thermal mass.

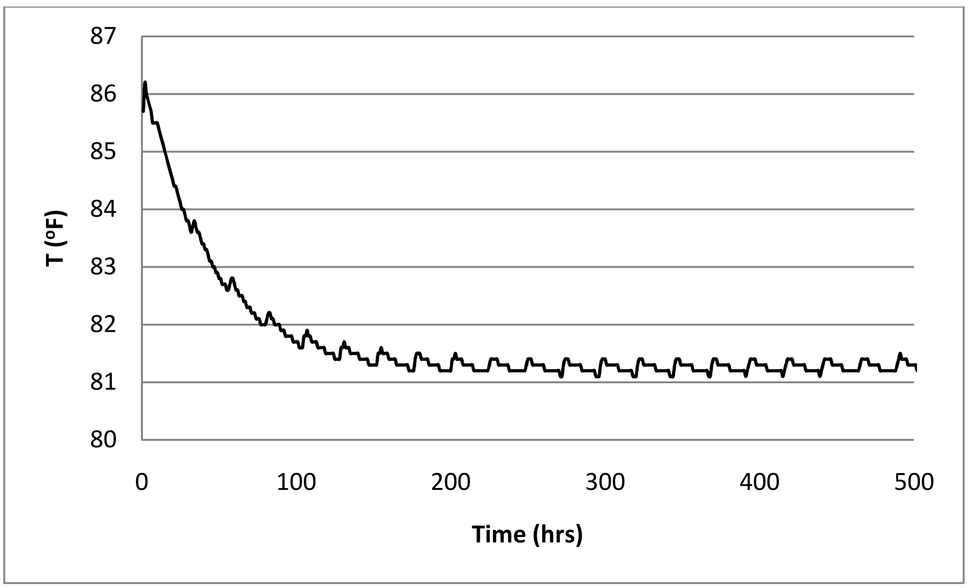

Figure 6.19 - Plot of the response function (indoor temperature) with increasing time period (minutes) predicted by the eQUEST simulation program.

Custom or standard weighting factor specifies the composite weight of the floor, furnishings, and interior walls of a space divided by the floor area of the space. The input value determines the weighting factors associated with the space. ASHRAE weighting factors are used. Higher input values give a longer lag time between heat gains and resultant cooling loads, and greater damping of peak loads. Internal mass or custom weighting factor comes into place only when the custom or standard weighting factor is zero. It takes a code-word that describes the thermal response of only the furniture in the space. The study used custom or standard weighting factor with floor weight of 85 lb/ft^2 to achieve the stated time constant of 26.8 hours.

7. CONCLUSIONS

The heat transfer model and thermal network model developed in this research will make it easier for the architects/ engineers to assess the potential of night ventilation as a strategy to implement in their specific location. A Discomfort Reduction Factor (DRF) is proposed as an index which provides such an assessment. From the calculated indoor temperature dynamics, the reduction in air-conditioning load may be estimated when night ventilation is used in conditioned buildings. Though these models are analyzed for a prototype small office building, the methodology used in analyzing and developing these models may be extrapolated to larger sized buildings. These models are relatively easy to use and provide a quick assessment. Using the software code developed, one is able to quickly determine the relevant performance measures (Indoor temperature and Discomfort Reduction Factor) with little computing effort. The expertise required to develop the models, generate and analyze the results are less than that required for performing whole building simulation models. Though the accuracy of results is slightly compromised, the loss in accuracy using these tools more than compensates for the insights such as analysis provides as well as the transparency in the analysis approach.

These models were used to evaluate the night ventilation effectiveness for two climate zones, Phoenix, AZ and Albuquerque, NM, for three time constants of 25 hrs, 15 hrs and 6 hrs and three peak air changes per hour (ACH) of 20, 10 and 5. It was observed that night ventilation is effective when day time ambient temperatures are between 36 ^{o}C and 30 ^{o}C and night time ambient temperatures below 20 ^{o}C. Implementing night ventilation between January to April and October to December are best for Phoenix, AZ when the weather is pleasant and not too hot. On the other hand, night ventilation strategy is more effective for Albuquerque, NM during the period April to October when its weather is pleasant and not cold. As expected, it was observed that DRFs increased with increase in time constants. 25 hrs of time constant resulted in higher DRFs compared to 15 hrs which, in turn, has greater DRFs compared to 6 hrs. Similar kind of results was observed with increase in ACH. DRF values predicted by the Heat Transfer model and the Thermal network model differ to some extent. This is due to the manner in which each of the models treat the coupling of thermal capacity of ventilation air with internal thermal mass and the methodology of solving the equations. The Heat Transfer used closed form solutions where as the Thermal Network model used numerical method. However, the patterns followed by monthly DRFs are similar and the variation in DRFs is minor. The results from these models are partially validated with whole building energy simulation program (eQUEST 3.64, 2010) and are closely concurrent.

8. RECOMMENDATIONS FOR FURTHER RESEARCH

This research can be further extended so as to make the models more accurate and useful. Recommendations for future research are stated below.

- Modifying the present thermal network to include more capacitors and resistors. Present thermal network is a one capacitor and four resistor network. More capacitors and resistors would make the model more realistic approximation of actual buildings. This will, however, increase the complexities of solving the thermal network model for generating the diurnal indoor temperature profile.
- Effect of heat gain from solar radiation should be considered in the models. Solar air properties should also be included.
- Sensitivity analysis of night ventilation effectiveness with thermal mass and volume of night ventilation air needs to be further investigated.
- The fan power required to implement the night ventilation strategy should be considered and the operation hours of ventilation optimized so as to minimize energy.
- These models and the methodology should be extended to air conditioned buildings so that estimates of the cooling energy reduction from night ventilation can be ascertained.

- Climatic mapping methodology of the cooling potential of night ventilation in residential and commercial buildings and its applications in arid climates should be explored.

9. REFERENCES

ANSI/ASHRAE Standard 55-2004. "Thermal Environmental Conditions for Human Occupancy", American Society of Heating Refrigeration and Air-conditioning Engineers, Atlanta, GA.

ANSI/ASHRAE Standard 62.1-2007. "Ventilation for Acceptable Indoor Air Quality", American Society of Heating Refrigeration and Air-conditioning Engineers, Atlanta, GA.

Artmann. N., R.L. Jensen, H. Manz and P. Heiselberg, 2010. "Experimental investigation of heat transfer during night-time ventilation". *Energy and Buildings*, vol. 42, pages 145-151.

ASHRAE TRP-1456, 2010. "Assess and implement natural and hybrid ventilation models in whole-building energy simulation", American Society of Heating Refrigeration and Air-conditioning Engineers, Atlanta, GA.

Buildings Energy Data Book, 2005. Office of Planning, Budget Formulation and Analysis, Energy Efficiency and Renewable Energy, U.S. Department of Energy.

Chalfoun N.V., 1997. "Design and Application of Natural Down-Draft Evaporative Cooling Devices", House Energy Doctor, UofA, Tuscon, http://hed.arizona.edu/.

eQUEST 3.64, 2010, http://doe2.com/download/DOE-22/DOE22Vol4-Libraries_44e2.pdf, James J. Hirsch

Feuermann, D. and W. Hawthorne, 1991. "On the potential and effectiveness of passive night ventilation cooling", Solar Energy for the 21st Century, proceedings of the 1991 Congress of ISES, Denver, CO, August 19th - 23rd.

Geros. V., M. Santamouris, A. Tsangrasoulis and G. Guarracino, 1999 "Experimental evaluation of night ventilation phenomena", *Energy and Buildings*, vol. 37, pages 243-257.

Givoni, B., 1994. *"Passive Low Energy Cooling of Buildings"*, John Wiley & Sons, Inc, Hoboken, NJ.

Givoni. B., 1998 "Effectiveness of mass and night ventilation in lowering the indoor daytime temperatures", *Energy and Buildings*, vol. 28, pages 25-32.

Kolokotroni. M. and A. Aronis, 1999 "Cooling-energy reduction in air-conditioned offices by using night ventilation", *Applied Energy*, vol. 63, pages 241-253.

Kreider J.F, P.S. Curtiss and A. Rabl, 2005, *"Heating and Cooling of Buildings, Design for Efficiency",* Second Edition, 2005. Kreider and Associates, Boulder, Colorado.

Lee. K.H. and R.K. Strand, 2008. "Enhancement of natural ventilation in buildings using a thermal chimney", Energy and Buildings, vol. 40, pages 214-220.

Nayak, J.K. and J.A. Prajapati, 2006. *"Handbook on Energy Conscious Buildings"*. Interactive R&D project between IIT, Bombay and Solar Energy Centre, MNRE, India.

Pfafferott. J., S. Herkel and M. Jäschke, 2003. "Design of passive cooling by night ventilation: evaluation of a parametric model and building simulation with measurements", *Energy and Buildings*, vol. 35, pages 1129–1143.

Reddy, T.A., 1989, "Identification of building parameters using dynamic inverse models: Analysis of three occupied residences monitored non-intrusively", Princeton, N.J. The Center for Energy and Environmental Studies.

Shaviv. E., A. Yezioro and I.G. Capeluto, 2001. "Thermal mass and night ventilation as passive cooling design strategy", *Renewable Energy*, vol. 24, pages 445-452.

TMY3 weather data, http://rredc.nrel.gov/solar/old_data/nsrdb/1991-2005/tmy3/

Yam, J., Y. Li and Z. Zhend, 2003. "Nonlinear coupling between thermal mass and natural ventilation in buildings", *International Journal of Heat and Mass Transfer*, vol. 46, pages 1251-1264.

Zhou, J., G. Zhang, Y. Lin and Y. Li, 2008. "Coupling of thermal mass and natural ventilation in buildings", *Energy and Buildings*, vol. 40, pages 979–986.

APPENDIX A

LISTING OF MATLAB CODE

Program 1 – Heat Transfer model

```
clear
clc
data=xlsread('data.xlsx'); % Reads weather data
va=xlsread('Variables.xlsx'); % Reads building data
no=size(data,1);
%Repeated hours for each day
p=1;
q=24;
for j=1:365
   time(p:q)=(1:24);
    p=p+24;
    q=q+24;
end
xlswrite('data.xlsx',time',1,'G2');
%loads for each day
% p=1;
% q=24;
for i=1:no
   Heat(i)=data(i,6);
%     p=p+24;
%     q=q+24;
end
xlswrite('data.xlsx',Heat',1,'H2');
%calculation exterior overall heat transfer coefficient
for i=1:no
OC(i)=((0.3*(data(i,5)*2.236936))+2.2)*5.6786;
end
xlswrite('data.xlsx',OC',1,'K2');
%Generating 1s when night ventilation is required or else 0s
 for i=1:no
if(data(i,7)>8 && data(i,7)<22)
  value(i)=0;
else
  value(i)=1;
  end
 end
 xlswrite('data.xlsx',value',1,'I2');

 %calculation Tamb mean and Tcomf
m=1;
n=730;
for j=1:12
   for i=m:n
       Tamean(i)=mean(data(m:n,4));
   end
   m=m+730;
   n=n+730;
end


for i=1:no
    if Tamean(i)>=10
Tcomf(i)=(0.26*Tamean(i))+15.5;
    elseif Tamean(i)<=34
```

```
        Tcomf(i)=(0.26*Tamean(i))+15.5;
    else
        Tcomf(i)=24
    end
end


for i=1:no
if(value(i)==1 && data(i,4)>Tcomf(i))
  value1(i)=0;
else
 value1(i)=value(i);
 end
 end
 xlswrite('data.xlsx',value1',1,'J2');
 for i=1:no
if(value1(i)==1 && data(i,4)<15)
  value2(i)=0;
else
 value2(i)=value1(i);
 end
 end
 xlswrite('data.xlsx',value2',1,'Z2');

 %Indoor overall heat transfer coefficient
for i=1:no
if(value2(i)==0)
  IC(i)=va(10,3);
else
    IC(i)=va(9,3);
end
end
xlswrite('data.xlsx',IC',1,'L2');
%Overall Resistance
for i=1:no
R(i)=((1/data(i,11))+(1/data(i,12))+va(5,1));
end
 xlswrite('data.xlsx',R',1,'M2');
 %Volume of air
 for i=1:no
if(value2(i)==0)
  Q(i)=va(10,2);
else
    Q(i)=va(9,2);
end
end
xlswrite('data.xlsx',Q',1,'N2');

% Finding Lambda

for i=1:no
Lambda(i)=(IC(i)*((4*va(1,1)*va(2,1))+(2*va(2,1)*va(3,1))))/(1.2*
1005*Q(i));
end
xlswrite('data.xlsx',Lambda',1,'O2');
```

```
%Finding timeconstnat

for i=1:no
if(value2(i)==0)
  TC(i)=va(10,7);
else
    TC(i)=va(9,7);
end
end
xlswrite('data.xlsx',TC',1,'P2');

%Finding Te

for i=1:no
Te(i)=(data(i,8)*(va(2,1)*va(3,1)))/(1.2*1005*Q(i));
end
xlswrite('data.xlsx',Te',1,'Q2');

%Mean To
p=1;
q=24;
for j=1:365
   To(p:q)=mean(data(p:q,4));
    p=p+24;
    q=q+24;
end
xlswrite('data.xlsx',To',1,'R2');

%Ao
p=1;
q=24;
for j=1:365
   Ao(p:q)=(max(data(p:q,4))-min(data(p:q,4)))/2;
    p=p+24;
    q=q+24;
end
xlswrite('data.xlsx',Ao',1,'S2');

for i=1:no
    if(value2(i)==0)
Ai(i)=Ao(i)*va(10,8);
    else
        Ai(i)=Ao(i)*va(9,8);
    end
end
xlswrite('data.xlsx',Ai',1,'T2');
%Mean Timean
for i=1:no
%
Timean(i)=(data(i,18)+data(i,17)+((data(i,15)/(data(i,13)*data(i,
12)))*data(i,4)))/((data(i,15)/(data(i,13)*data(i,12))));
Timean(i)=(To(i)+Te(i)+((Lambda(i)/(R(i)*IC(i)))*data(i,4)))/(1+(
Lambda(i)/(R(i)*IC(i))));
end
xlswrite('data.xlsx',Timean',1,'U2');
%Finding Ti
```

```
for i=1:no
    if(value2(i)==0)
Ti(i)= Timean(i)+(Ai(i)*cos((pi/12)*(data(i,7)-va(10,9))));
    else
        Ti(i)= Timean(i)+(Ai(i)*cos((pi/12)*(data(i,7)-
va(9,9))));
    end
end
xlswrite('data.xlsx',Ti',1,'V2');

%no NV

for i=1:no
    if(value2(i)==0)
    Qno(i)=va(13,2);
    else
    Qno(i)=va(12,2);
    end
end
for i=1:no
    if(value2(i)==0)
    ICno(i)=va(13,3);
    else
        ICno(i)=0;
    end
end
for i=1:no
    if(value2(i)==0)
Rno(i)=((1/data(i,11))+(1/ICno(i))+va(5,1));
    else
        Rno(i)=0;
    end
end
for i=1:no
    if(value2(i)==0)

Lambdano(i)=(ICno(i)*((4*va(1,1)*va(2,1))+(2*va(2,1)*va(3,1))))/(
1.2*1005*Qno(i));
else
    Lambdano(i)=0;
end
%
Lambdano(i)=(ICno(i)*((4*va(1,1)*va(2,1))+(2*va(2,1)*va(3,1))))/(
1.2*1005*Qno(i));
end
xlswrite('data.xlsx',Lambdano',1,'W2');

for i=1:no
    Teno(i)=(data(i,8)*(va(2,1)*va(3,1)))/(1.2*1005*Qno(i));
end
for i=1:no
    if(value2(i)==0)
Timeanno(i)=(To(i)+Teno(i)+((Lambdano(i)/(Rno(i)*ICno(i)))*data(i
,4)))/(1+(Lambdano(i)/(Rno(i)*ICno(i))));
    else
        Timeanno(i)=To(i)+Teno(i);
```

```
    end
end
xlswrite('data.xlsx',Timeanno',1,'X2');
for i=1:no
    if(value2(i)==0)
Ai(i)=Ao(i)*va(13,8);
    else
        Ai(i)=Ao(i)*va(12,8);
    end
end
for i=1:no
    if(value2(i)==0)
Tino(i)= Timeanno(i)+(Ai(i)*cos((pi/12)*(data(i,7)-va(13,9))));
    else
        Tino(i)= Timeanno(i)+(Ai(i)*cos((pi/12)*(data(i,7)-
va(12,9))));
    end
end
xlswrite('data.xlsx',Tino',1,'Y2');

%cooling efficency


for i=1:no
    if((Tino(i)-Tcomf(i))>=0)
        nopos(i)=(Tino(i)-Tcomf(i));
    else
        nopos(i)=0;
    end
    if((Ti(i)-Tcomf(i))>=0)
        pos(i)=(Ti(i)-Tcomf(i));
    else
        pos(i)=0;
    end
end

p=1;
q=24;
for j=1:365
    if (sum(nopos(p:q))<=sum(pos(p:q)))
        CE(p:q)=0;
        CEgraph(j)=0;
    elseif(max(Ti(p:q))<=20)
        CE(p:q)=0;
        CEgraph(j)=0;
    elseif(sum(nopos(p:q))==0)
        CE(p:q)=0;
        CEgraph(j)=0;
        else
   CE(p:q)=(sum(nopos(p:q))-sum(pos(p:q)))/sum(nopos(p:q));
   CEgraph(j)=(sum(nopos(p:q))-sum(pos(p:q)))/sum(nopos(p:q));
    end
    p=p+24;
    q=q+24;
end
% for i=1:no
```

```
%     CE(i)=(nopos(i)-pos(i))/nopos(i);
% end
xlswrite('data.xlsx',CE',1,'AB2');
xlswrite('data.xlsx',CEgraph',1,'AC2');

%Aggregate DRF
a=1;
b=730;
for j=1:12
   if (sum(nopos(a:b))<=sum(pos(a:b)))
        CEagg(a:b)=0;
        CEagggraph(j)=0;
    elseif(max(Ti(a:b))<=18)
        CEagg(a:b)=0;
        CEagggraph(j)=0;
    elseif(sum(nopos(a:b))==0)
        CEagg(a:b)=0;
        CEagggraph(j)=0;
        else
   CEagg(a:b)=(sum(nopos(a:b))-sum(pos(a:b)))/sum(nopos(a:b));
   CEagggraph(j)=(sum(nopos(a:b))-sum(pos(a:b)))/sum(nopos(a:b));
    end
   a=a+730;
   b=b+730;
end
% a=1;
% b=30;
% for j=1:12
%     CEaggregate(j)=sum(CEgraph(a:b));
%     a=a+30;
%     b=b+30;
% end
xlswrite('data.xlsx',CEagggraph',1,'AE2');
```

Program 2 – Thermal Network model

```
clear
clc
data=xlsread('data.xlsx'); Reads weather data
val=xlsread('variables1.xlsx'); % Reads building data
no=size(data,1);
%Repeated hours for each day
p=1;
q=24;
for j=1:365
   time(p:q)=(1:24);
    p=p+24;
    q=q+24;
end
xlswrite('data.xlsx',time',1,'G2');
%Repeated loads for each day

%calculation Tamb mean
m=1;
```

```
n=730;
for j=1:12
   for i=m:n
       Tamean(i)=mean(data(m:n,4));
   end
   m=m+730;
   n=n+730;
end

for i=1:no
    if Tamean(i)>=10
Tcomf(i)=(0.26*Tamean(i))+15.5;
    elseif Tamean(i)<=34
        Tcomf(i)=(0.26*Tamean(i))+15.5;
    else
        Tcomf(i)=24
    end
end


p=1;
q=24;
for i=1:no
   Qa(i)=data(i,6);
%     p=p+24;
%     q=q+24;
Qa(i)=Qa(i)*232.26;
end
xlswrite('data.xlsx',Qa',1,'H2');
%calculation exterior overall heat transfer coefficient
for i=1:no
OC(i)=((0.3*(data(i,5)*2.236936))+2.2)*5.6786;
end
xlswrite('data.xlsx',OC',1,'L2');
%Generating 1s when night ventilation is required or else 0s
 for i=1:no
if(data(i,7)>8 && data(i,7)<22)
  value(i)=0;
else
  value(i)=1;
  end
 end
 xlswrite('data.xlsx',value',1,'I2');
for i=1:no
if(value(i)==1 && data(i,4)>Tcomf(i))
  value1(i)=0;
else
 value1(i)=value(i);
 end
 end
 xlswrite('data.xlsx',value1',1,'J2');
 for i=1:no
if(value1(i)==1 && data(i,4)<15)
  value2(i)=0;
else
 value2(i)=value1(i);
```

```
 end
 end
 xlswrite('data.xlsx',value2',1,'K2');

 %Volume of air
 for i=1:no
if(value2(i)==0)
  Q(i)=val(10,2);
else
    Q(i)=val(9,2);
end
end
xlswrite('data.xlsx',Q',1,'M2');

%Resistance between Tambient and Tindoor

 for i=1:no
R1(i)=1/((1/(OC(i)*val(4,1))+ val(5,1))+ (1.2*1005*Q(i)));
end
xlswrite('data.xlsx',R1',1,'N2');


 %Indoor overall heat transfer coefficient
for i=1:no
if(value2(i)==0)
  IC(i)=val(10,3);
else
    IC(i)=val(9,3);
end
end
xlswrite('data.xlsx',IC',1,'O2');

%Resistance between Tambient and Tindoor
for i=1:no
R2(i)=1/(IC(i)*val(4,1));
end
xlswrite('data.xlsx',R2',1,'P2');

%Finding capacitance
C=val(6,1);

%Input of Qs
for i=1:no
    Qs(i)=data(i,17);
end

% Finding ao,b1,co,c1,d1
for i=1:no
ao(i)=R2(i)/(R1(i)*(1+(R2(i)/R1(i))));
b1(i)=1/(val(6,1)*R1(i)*(1+(R2(i)/R1(i))));
co(i)=R2(i)/(1+(R2(i)/R1(i)));
c1(i)=1/(val(6,1)*(1+(R2(i)/R1(i))));
% d1(i)=val(7,1)/(val(6,1)*(1+(R2(i)/R1(i))));
d1(i)=0;
end
```

```
%Input of Ta
for i=1:no
    Ta(i)=data(i,4);
end
Ti(1)=data(1,18);

%Finding Ti
for i=2:no
    Ti(i)=((ao(i)*(Ta(i)-Ta(i-1)))+(b1(i)*1800*(Ta(i)+Ta(i-1)-
Ti(i-1)))+(co(i)*(Qa(i)-Qa(i-1)))+(c1(i)*1800*(Qa(i)+Qa(i-
1)))+(d1(i)*1800*(Qs(i)+Qs(i-1)))+Ti(i-1))/(1+(1800*b1(i)));
end
xlswrite('data.xlsx',Ti',1,'R2');


%no NV

for i=1:no
    if(value2(i)==0)
    Qno(i)=val(13,2);
    else
    Qno(i)=val(12,2);
    end
end

for i=1:no
R1no(i)=1/((OC(i)*val(4,1))+(1/val(5,1))+(1.2*1005*Qno(i)));
end
for i=1:no
    if(value2(i)==0)
    ICno(i)=val(13,3);
    else
        ICno(i)=0;
    end
end
for i=1:no
    if(value2(i)==0)
    R2no(i)=1/(ICno(i)*val(4,1));
%     else
%         R2no(i)=0;
    end
end

for i=1:no
aono(i)=R2no(i)/(R1no(i)*(1+(R2no(i)/R1no(i))));
b1no(i)=1/(val(6,1)*R1no(i)*(1+(R2no(i)/R1no(i))));
cono(i)=R2no(i)/(1+(R2no(i)/R1no(i)));
c1no(i)=1/(val(6,1)*(1+(R2no(i)/R1no(i))));
% d1no(i)=val(7,1)/(val(6,1)*(1+(R2no(i)/R1no(i))));
d1no(i)=0;
end

Tino(1)=data(1,18);
```

```
for i=2:no
    Tino(i)=((aono(i)*(Ta(i)-Ta(i-1)))+(b1no(i)*1800*(Ta(i)+Ta(i-
1)-Tino(i-1)))+(cono(i)*(Qa(i)-Qa(i-
1)))+(c1no(i)*1800*(Qa(i)+Qa(i-1)))+(d1no(i)*1800*(Qs(i)+Qs(i-
1)))+Tino(i-1))/(1+(1800*b1no(i)));
end
xlswrite('data.xlsx',Tino',1,'S2');

%calculation Tamb mean
m=1;
n=730;
for j=1:12
   for i=m:n
       Tamean(i)=mean(data(m:n,4));
   end
   m=m+730;
   n=n+730;
end

for i=1:no
    if Tamean(i)>=10
Tcomf(i)=(0.26*Tamean(i))+15.5;
    elseif Tamean(i)<=34
        Tcomf(i)=(0.26*Tamean(i))+15.5;
    else
        Tcomf(i)=24
    end
end

%cooling efficency
% Tcomf=24;
for i=1:no
    if((Tino(i)-Tcomf(i))>=0)
        nopos(i)=(Tino(i)-Tcomf(i));
    else
        nopos(i)=0;
    end
    if((Ti(i)-Tcomf(i))>=0)
        pos(i)=(Ti(i)-Tcomf(i));
    else
        pos(i)=0;
    end
end
%finding temp difference
for i=1:no
    Tdef(i)=Tino(i)-Ti(i);
end
xlswrite('data.xlsx',Tdef',1,'T2');


p=1;
q=24;
for j=1:365
    if (sum(nopos(p:q))<=sum(pos(p:q)))
        CE(p:q)=0;
        CEgraph(j)=0;
```

```
     elseif(max(Ti(p:q))<=18)
         CE(p:q)=0;
         CEgraph(j)=0;
     elseif(sum(nopos(p:q))==0)
         CE(p:q)=0;
         CEgraph(j)=0;
         else
    CE(p:q)=(sum(nopos(p:q))-sum(pos(p:q)))/sum(nopos(p:q));
    CEgraph(j)=(sum(nopos(p:q))-sum(pos(p:q)))/sum(nopos(p:q));
     end
     p=p+24;
     q=q+24;
end
% for i=1:no
%     CE(i)=(nopos(i)-pos(i))/nopos(i);
% end
xlswrite('data.xlsx',CE',1,'U2');
xlswrite('data.xlsx',CEgraph',1,'V2');

%Aggregate CE
a=1;
b=730;
for j=1:12
   if (sum(nopos(a:b))<=sum(pos(a:b)))
         CEagg(a:b)=0;
         CEagggraph(j)=0;
     elseif(max(Ti(a:b))<=20)
         CEagg(a:b)=0;
         CEagggraph(j)=0;
     elseif(sum(nopos(a:b))==0)
         CEagg(a:b)=0;
         CEagggraph(j)=0;
         else
   CEagg(a:b)=(sum(nopos(a:b))-sum(pos(a:b)))/sum(nopos(a:b));
   CEagggraph(j)=(sum(nopos(a:b))-sum(pos(a:b)))/sum(nopos(a:b));
     end
   a=a+730;
   b=b+730;
end
% a=1;
% b=30;
% for j=1:12
%     CEaggregate(j)=sum(CEgraph(a:b));
%     a=a+30;
%     b=b+30;
% end
xlswrite('data.xlsx',CEagggraph',1,'X2');
% xlswrite('data.xlsx',CEaggregate',1,'X2');
```